

Subwavelength resonances in 1D high-contrast acoustic media

F. Feppon and Z. Cheng and H. Ammari

Research Report No. 2022-29
June 2022

Seminar für Angewandte Mathematik
Eidgenössische Technische Hochschule
CH-8092 Zürich
Switzerland

SUBWAVELENGTH RESONANCES IN 1D HIGH-CONTRAST ACOUSTIC MEDIA

F. FEPPON¹, Z. CHENG¹ AND H. AMMARI¹

¹*Department of Mathematics, ETH Zürich, Switzerland.*

ABSTRACT. We propose a mathematical theory of acoustic wave scattering in one-dimensional finite high-contrast media. The system considered is constituted of a finite alternance of high-contrast segments of arbitrary lengths and interdistances, called the “resonators”, and a background medium. We prove the existence of subwavelength resonances, which are the counterparts of the well-known Minnaert resonances in 3D systems. Our main contribution is to show that the resonant frequencies, as well as the transmission and reflection properties of the system can be accurately predicted by a “capacitance” eigenvalue problem, analogously to the 3D setting. Numerical results considering different situations with $N = 1$ to $N = 6$ resonators are provided to support our mathematical analysis, and to illustrate the various possibilities offered by high-contrast resonators to manipulate waves at subwavelength scales.

Keywords. Acoustic waves, subwavelength resonances, high-contrast, one-dimensional media, transmission coefficient.

AMS Subject classifications. 35B34, 35P25, 35J05, 35C20, 46T25, 78A40.

CONTENTS

1. Introduction	1
2. The Dirichlet-to-Neumann map in one dimension	5
3. Subwavelength resonances in 1D acoustic media	7
3.1. A first characterization of resonances based on an explicit representation of the solution	8
3.2. Characterization of the resonances based on the Dirichlet-to-Neumann approach	8
3.3. Asymptotic expansions of the subwavelength resonances	10
4. Modal decompositions and transmission properties in the high-contrast medium	14
4.1. Modal decomposition of the wave total field	14
4.2. Transmission and reflection coefficients of the high-contrast medium	17
5. Numerical illustrations of subwavelength resonances	19
5.1. Setting and methodology	19
5.2. Single resonator case	20
5.3. Two resonator case	20
5.4. Six resonator case	22
5.5. Six resonator case with perfect transmission	25
References	31

1. INTRODUCTION

High-contrast media have raised a lot of attention in the field of photonics and phononics thanks to their ability to manipulate waves at subwavelength scales [21, 20, 23, 24]. These media are constituted of a background medium and a set of highly contrasted bounded inclusions. The high-contrast property gives rise to “subwavelength” resonances, which are frequencies at which the resonators strongly interact with incident waves whose wavelengths can be larger by several orders of magnitude. A typical example of such high-contrast systems are air bubbles in water, where the associated subwavelength resonances are called Minnaert resonances [29]. Subwavelength resonances also arise in high-contrast elastic media [25], in plasmonic particles [10], or in Helmholtz resonators [22]; they enable to achieve a variety of wave applications such as superfocusing [19], cloaking [1] or guiding [5].

Mathematically, subwavelength resonances correspond to complex poles of the solution operator of the system: they are a particular type of “scattering resonances” [37] encountered in quantum physics. The scattered field is significantly amplified as the real incident frequency $\omega \in \mathbb{R}$ becomes close to the complex resonant frequency; the imaginary part of the resonance is usually small and its physically stems from the radiation of energy at

* Corresponding author. Email: florian.feppon@sam.math.ethz.ch.

The work of F. Feppon was supported by ETH Zürich through the Hermann-Weyl fellowship of the Institute for Mathematical Research (FIM)..

infinity. Furthermore, these poles are called “subwavelength” frequencies because they lie in a small complex neighborhood of the origin; this property allows to study them by mean of some asymptotic analysis in the regime $\omega \rightarrow 0$.

So far, high-contrast resonant scattering has been thoroughly investigated mostly in the three-dimensional setting [8, 13, 28, 2, 4, 15], which is somewhat the “easiest case” due to the decay properties of the fundamental solution to the Helmholtz equation. We can only mention [8] which consider a single high-contrast inclusion in a 2D setting, and [6, 3] who considered an infinitely periodic 1D chain of three-dimensional subwavelength resonators. There has been recently, though, a rise of interest in the analysis of the topological properties of one-dimensional, infinitely periodic wave systems: [26] considered resonances in finite photonic crystals with a defect, [27] considered 1D infinitely periodic media with continuous physical parameters, while [12] studies a simplified SSH model with piecewise continuous physical parameters. Beside these references, we can mention the work of [18] who considered the optimization of scattering resonances in a finite chain of 1D resonators. Subwavelength resonant 1D systems have also been studied through physical experiments [11, 33, 36, 35], which were observed to possess exceptional acoustic or optical transmission properties near resonant frequencies. However, to the best of our knowledge, a rigorous mathematical analysis of the resonances in acoustic scattering of one-dimensional waves seems still to be missing from the literature.

The purpose of this paper is therefore to propose a complete mathematical analysis of subwavelength resonances to one-dimensional, high-contrast, finite media. Of particular interest, an analogy between systems of subwavelength resonators and systems of particles in quantum physics, where the tight-binding model is often used, is shown. We consider a system $D = \bigsqcup_{i=1}^N (x_i^-, x_i^+)$ constituted of a chain of N disjoint subwavelength resonators (x_i^-, x_i^+) , where $(x_i^\pm)_{1 \leq i \leq N}$ are the $2N$ extremities satisfying $x_i^+ < x_{i+1}^-$ for any $0 \leq i \leq N-1$. We denote by $\ell_i = x_i^+ - x_i^-$ the length of the i -th resonator, and by $\ell_{i(i+1)} = x_{i+1}^- - x_i^+$ the length of the gap between the i -th and $(i+1)$ -th resonator. The system is illustrated on Figure 1.

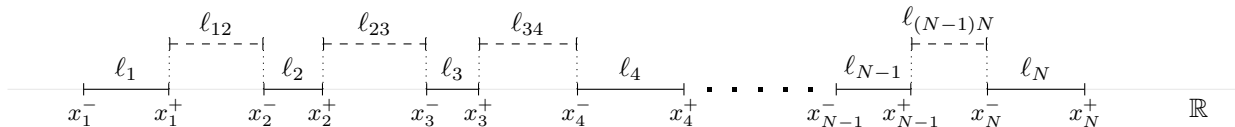


FIGURE 1. A system of N subwavelength resonators, with lengths $(\ell_i)_{1 \leq i \leq N}$ and interdistances $(\ell_{i(i+1)})_{1 \leq i \leq N-1}$.

An acoustic wave field $u(t, x)$ propagates in the heterogeneous medium, which is solution to the 1D wave equation:

$$\frac{1}{\kappa(x)} \frac{d^2}{dt^2} u(t, x) - \frac{d}{dx} \left(\frac{1}{\rho(x)} \frac{d}{dx} u(t, x) \right) = 0, \quad (t, x) \in \mathbb{R} \times \mathbb{R}. \quad (1.1)$$

The parameters $\kappa(x)$ and $\rho(x)$ are respectively the acoustic bulk modulus and the density of the medium, given by

$$\kappa(x) = \begin{cases} \kappa_b & \text{if } x \in D, \\ \kappa & \text{if } x \in \mathbb{R} \setminus D, \end{cases} \quad \rho(x) = \begin{cases} \rho_b & \text{if } x \in D, \\ \rho & \text{if } x \in \mathbb{R} \setminus D. \end{cases} \quad (1.2)$$

The total wave field $u(t, x)$ is assumed to be time-harmonic, and is decomposed as the sum of a prescribed incident wave and an “unknown” outgoing scattered wave:

$$u(t, x) = e^{-i\omega t} u(x) \text{ with } u(x) = u_{\text{in}}(x) + u_s(x). \quad (1.3)$$

The incident wave u_{in} is time-harmonic with frequency ω ; it satisfies:

$$\left(\frac{d^2}{dx^2} + k^2 \right) u_{\text{in}} = 0 \text{ in } \mathbb{R}, \quad (1.4)$$

where, following the notation of [8, 15], the wave speeds inside the resonators D and inside the background medium $\mathbb{R}^3 \setminus D$, are denoted respectively by v_b and v , the wave numbers respectively by k_b and k , and the contrast between the resonators and the background medium by δ :

$$v_b := \sqrt{\frac{\kappa_b}{\rho_b}}, \quad v := \sqrt{\frac{\kappa}{\rho}}, \quad k_b := \frac{\omega}{v_b}, \quad k := \frac{\omega}{v}, \quad \delta := \frac{\rho_b}{\rho}.$$

On the other hand, the scattered wave $(t, x) \mapsto e^{-i\omega t} u_s(x)$ is determined by the fact that it should be “outgoing”, i.e. that it should be a function of $t - |x|/v$. Since u_s must satisfy $(\frac{d^2}{dx^2} + k^2)u_s = 0$ far away from D , “outgoing” means in the 1D setting that $u_s(x)$ must be proportional to $e^{ik|x|}$ for $|x|$ sufficiently large (more precisely, for

$x < x_1^-$ and for $x > x_N^+$). This can equivalently be rewritten in the form of the following Sommerfeld radiation condition for u_s :

$$\left(\frac{d}{d|x|} - ik \right) u_s = 0 \text{ for } x \in (-\infty, x_1^-) \cup (x_N^+, +\infty). \quad (1.5)$$

In these circumstances, the wave problem determined by (1.1) and (1.5) can be rewritten as the following coupled system of 1D Helmholtz equations:

$$\left\{ \begin{array}{ll} \frac{d^2}{dx^2} u + \frac{\omega^2}{v^2} u = 0 & \text{in } \mathbb{R} \setminus \bigcup_{i=1}^N (x_i^-, x_i^+), \\ \frac{d^2}{dx^2} u + \frac{\omega^2}{v_b^2} u = 0 & \text{in } \bigcup_{i=1}^N (x_i^-, x_i^+), \\ u|_-(x_i^\pm) = u|_+(x_i^\pm) & \text{for all } 1 \leq i \leq N, \\ \frac{du}{dx} \Big|_+ (x_i^-) = \delta \frac{du}{dx} \Big|_- (x_i^-) & \text{for all } 1 \leq i \leq N, \\ \frac{du}{dx} \Big|_- (x_i^+) = \delta \frac{du}{dx} \Big|_+ (x_i^+) & \text{for all } 1 \leq i \leq N, \\ \left(\frac{d}{d|x|} - ik \right) (u - u_{\text{in}}) = 0 & \text{for } x \in (-\infty, x_1^-) \cup (x_N^+, +\infty), \end{array} \right. \quad (1.6)$$

where for a 1D function w , we have denoted

$$w|_-(x) = \lim_{\substack{s \rightarrow 0 \\ s > 0}} w(x - s), \quad w|_+(x) = \lim_{\substack{s \rightarrow 0 \\ s > 0}} w(x + s).$$

We study subwavelength resonances for the scattering problem (1.6) by performing an asymptotic analysis in the low-frequency and high-contrast regimes

$$\omega \rightarrow 0, \quad \delta \rightarrow 0. \quad (1.7)$$

The mathematical analysis for the three-dimensional counterpart of (1.6) states that a system of N high-contrast connected inclusions $D = \bigcup_{i=1}^N D_i$ admits exactly $2N$ subwavelength resonant frequencies $(\omega_i^\pm(\delta))_{1 \leq i \leq N}$ [2, 15]. Moreover, the leading-order asymptotic of these resonant frequencies is given by

$$\omega_i^\pm(\delta) \sim \pm v_b \lambda_i^{\frac{1}{2}} \delta^{\frac{1}{2}}, \quad 1 \leq i \leq N, \quad (1.8)$$

where $(\lambda_i)_{1 \leq i \leq N}$ are the N eigenvalues of a symmetric eigenvalue problem [2, 15] with eigenvectors $(\mathbf{a}_i)_{1 \leq i \leq N}$, which read

$$C \mathbf{a}_i = \lambda_i V \mathbf{a}_i, \quad 1 \leq i \leq N. \quad (1.9)$$

The matrix V is the diagonal matrix gathering the volumes of the resonators, $V = \text{diag}(|D_i|)_{1 \leq i \leq N}$, while C is the so-called ‘‘capacitance matrix’’, whose entries can be defined by the formula

$$C_{ij} := - \int_{\partial D_i} \frac{\partial u_j}{\partial n} d\sigma \quad \text{with} \quad \left\{ \begin{array}{l} -\Delta u_i = 0 \text{ in } \mathbb{R}^3 \setminus \bigcup_{l=1}^N D_l, \\ u_i = \delta_{ij} \text{ on } \partial D_j, \\ u_i(x) = O(|x|^{-1}) \text{ as } |x| \rightarrow +\infty. \end{array} \right. \quad 1 \leq i, j \leq N. \quad (1.10)$$

One of the main contributions of the present paper is to show that a capacitance formalism analogous to (1.9) exists in 1D, up to some differences which are now described. First, the ‘‘capacitance’’ matrix in 1D should be defined as

$$C_{ij} := - \left(- \frac{du_i}{dx}(x_j^-) + \frac{du_i}{dx}(x_j^+) \right) \quad \text{with} \quad \left\{ \begin{array}{l} - \frac{d^2}{dx^2} u_i = 0 \text{ in } \mathbb{R} \setminus \bigcup_{l=1}^N (x_l^-, x_l^+), \\ u_i(x_j^\pm) = \delta_{ij}, \\ u_i(x) = O(1) \text{ as } |x| \rightarrow +\infty, \end{array} \right. \quad 1 \leq i, j \leq N, \quad (1.11)$$

which is the direct analogue of (1.10) up to the adaptation of the decay condition at infinity (in fact $u_i(x)$ is even constant for $x \leq x_1^-$ or $x \geq x_N^+$). Solving explicitly (1.11) (the solution u_i is plotted on Figure 2) yields the following expression for C_{ij} :

$$C_{ij} := - \frac{1}{\ell_{(j-1)j}} \delta_{i(j-1)} + \left(\frac{1}{\ell_{(j-1)j}} + \frac{1}{\ell_{j(j+1)}} \right) \delta_{ij} - \frac{1}{\ell_{j(j+1)}} \delta_{i(j+1)}, \quad 1 \leq i, j \leq N, \quad (1.12)$$

with the convention $1/\ell_{ij} = 0$ for indices i, j negative or greater than N . In other words, $C \equiv (C_{ij})_{1 \leq i, j \leq N}$ is

Helmholtz operator on the exterior domain $\mathbb{R} \setminus \overline{D}$. In [Section 3](#), we show the existence of $2N$ subwavelength resonances for the scattering problem [\(1.6\)](#), and we relate their asymptotic expansion to the capacitance eigenvalue problem [\(1.9\)](#); see [Proposition 3.3](#). In [Section 4](#), we establish a modal decomposition for the wave field $u(x)$ in the subwavelength regime [\(1.7\)](#), and we find asymptotics for the transmission and reflection coefficients of the system. Finally, [Section 5](#) presents a variety of numerical illustrations supporting our mathematical analysis of subwavelength resonances in 1D high-contrast media.

Before proceeding, we would like to highlight that this work leaves interesting connexions to explore with the ‘‘tight-binding’’ method of condensed matter physics [\[7\]](#). There is indeed an analogy between subwavelength resonators and particles in quantum physics, whose wave functions are solution to an eigenvalue problem analogous to [\(1.6\)](#). The tight-binding approach consists in approximating wave functions associated to several particles by a superposition of the modes associated to isolated particles, and to possibly add terms to take into account neighboring interactions [\[17, 32, 14\]](#).

From the point of view of acoustic waves, the capacitance matrix plays a role analogous to the Hamiltonian of quantum physics. In 3D, it is known that long-range interactions between a large number of particles cannot be neglected, because the coefficients of the capacitance matrix decay slowly away from the diagonal [\[6\]](#). However, such approximation would be exact in our one-dimensional context, due to the tridiagonal structure of the capacitance matrix.

2. THE DIRICHLET-TO-NEUMANN MAP IN ONE DIMENSION

In this section, we characterize the Dirichlet-to-Neumann map of the Helmholtz operator in one dimension, in view of applying the Dirichlet-to-Neumann approach of [\[16\]](#) for analyzing subwavelength resonances. We give a fully explicit expression of this operator in [Proposition 2.1](#), before computing its leading-order asymptotic expansion in [Corollary 2.1](#).

In all what follows, we denote by $H^1(D)$ the usual Sobolev space of complex-valued functions on D and by $H^{-1}(D)$ its dual space. Throughout the paper, we consider boundary data $f \equiv (f_i^\pm)_{1 \leq i \leq N} \in \mathbb{C}^{2N}$ with $2N$ components associated to the $2N$ points $(x_i^\pm)_{1 \leq i \leq N}$, where for any $1 \leq i \leq N$, we denote by f_i^+ (resp. f_i^-) the component associated to x_i^+ (resp. to x_i^-). The following lemma provides an explicit expression for the solution to exterior problems on $\mathbb{R} \setminus D$.

Lemma 2.1. *Assume that k is not of the form $k = n\pi/\ell_{i(i+1)}$ for some non-zero integer $n \in \mathbb{Z} \setminus \{0\}$ and index $1 \leq i \leq N - 1$. Then for any vector $(f_i^\pm)_{1 \leq i \leq N} \in \mathbb{C}^{2N}$, there exists a unique solution $w_f \in H_{\text{loc}}^1(\mathbb{R})$ to the exterior problem:*

$$\begin{cases} \left(\frac{d^2}{dx^2} + k^2 \right) w_f = 0 & \text{in } \mathbb{R} \setminus \bigsqcup_{i=1}^N (x_i^-, x_i^+), \\ w_f(x_i^\pm) = f_i^\pm & \text{for all } 1 \leq i \leq N, \\ \left(\frac{d}{d|x|} - ik \right) w_f(x) = 0 & \text{for } x \leq x_1^- \text{ or } x \geq x_N^+. \end{cases} \quad (2.1)$$

When further, $k \neq 0$, the solution w_f reads explicitly

$$w_f(x) = \begin{cases} f_1^- e^{-ik(x-x_1^-)} & \text{if } x \leq x_1^-, \\ a_i e^{ikx} + b_i e^{-ikx} & \text{if } x \in (x_i^+, x_{i+1}^-), \\ f_N^+ e^{ik(x-x_N^+)} & \text{if } x \geq x_N^+, \end{cases} \quad (2.2)$$

where a_i and b_i are given by the matrix-vector product

$$\begin{pmatrix} a_i \\ b_i \end{pmatrix} = -\frac{1}{2i \sin(k\ell_{i(i+1)})} \begin{pmatrix} e^{-ikx_{i+1}^-} & -e^{-ikx_i^+} \\ -e^{ikx_{i+1}^-} & e^{ikx_i^+} \end{pmatrix} \begin{pmatrix} f_i^+ \\ f_{i+1}^- \end{pmatrix}. \quad (2.3)$$

Proof. When $k \neq 0$, the solution w_f to [\(2.1\)](#) can be written as a linear combination of e^{ikx} and e^{-ikx} in each of the intervals $(x_i^+, x_{i+1}^-)_{1 \leq i \leq N-1}$ and may be represented as

$$w_f(x) = a_i e^{ikx} + b_i e^{-ikx}, \quad x \in (x_i^+, x_{i+1}^-). \quad (2.4)$$

The constants a_i and b_i are characterized from the boundary conditions of [\(2.1\)](#) at x_i^+ and x_{i+1}^- , which read:

$$\begin{cases} a_i e^{ikx_i^+} + b_i e^{-ikx_i^+} = f_i^+, \\ a_i e^{ikx_{i+1}^-} + b_i e^{-ikx_{i+1}^-} = f_{i+1}^-. \end{cases} \quad (2.5)$$

Inverting this system, we find the expression [\(2.3\)](#) for a_i and b_i . On the other hand, $w_f(x)$ must be proportional to e^{ikx} for $x > x_N^+$, and to e^{-ikx} for $x < x_1^-$, which yields [\(2.2\)](#).

If $k = 0$, it is obvious that [Lemma 2.1](#) admits a unique solution which is piecewise affine on each interval (x_i^+, x_{i+1}^-) for $1 \leq i \leq N-1$, and which is constant on the intervals $(-\infty, x_1^-)$ and $(x_N^+, +\infty)$. \square

Definition 2.1. For any $k \in \mathbb{C}$ which is not of the form $n\pi/\ell_{i(i+1)}$ for some $n \in \mathbb{Z} \setminus \{0\}$ and $1 \leq i \leq N-1$, the Dirichlet-to-Neumann map with wave number k is the linear operator $\mathcal{T}^k : \mathbb{C}^{2N} \rightarrow \mathbb{C}^{2N}$ defined by

$$\mathcal{T}^k[(f_i^\pm)_{1 \leq i \leq N}] = \left(\pm \frac{dw_f}{dx}(x_i^\pm) \right)_{1 \leq i \leq N}, \quad (2.6)$$

where w_f is the unique solution to [\(2.1\)](#).

Remark 2.1. The condition that $k \in \mathbb{C}$ is not of the form $n\pi/\ell_{i(i+1)}$ for some $n \in \mathbb{Z} \setminus \{0\}$ and $1 \leq i \leq N-1$ is equivalent to state that k^2 is not a Dirichlet eigenvalue of $-d^2/dx^2$ on $\mathbb{R} \setminus D$.

Remark 2.2. We consider a minus sign in [\(2.6\)](#) on the abscissa x_i^- because $\mathcal{T}^k[(f_j^\pm)_{1 \leq j \leq N}]_i^\pm$ is the “normal derivative” of w_f at x_i^\pm , with the normal pointing *outward* the segment (x_i^-, x_i^+) . This convention allows to maintain some analogy with the analysis in the 3D setting considered in [\[16, Section 3\]](#).

In the next proposition, we compute \mathcal{T}^k explicitly.

Proposition 2.1. *The Dirichlet-to-Neumann map \mathcal{T}^k admits the following explicit matrix representation: for any $k \in \mathbb{C} \setminus \{n\pi/\ell_{i(i+1)} \mid n \in \mathbb{Z} \setminus \{0\}, 1 \leq i \leq N-1\}$, $f \equiv (f_i^\pm)_{1 \leq i \leq N}$, $\mathcal{T}^k[f] \equiv (\mathcal{T}^k[f]_i^\pm)_{1 \leq i \leq N}$ is given by*

$$\begin{pmatrix} \mathcal{T}^k[f]_1^- \\ \mathcal{T}^k[f]_1^+ \\ \vdots \\ \mathcal{T}^k[f]_N^- \\ \mathcal{T}^k[f]_N^+ \end{pmatrix} = \begin{pmatrix} ik & & & & & \\ & A^k(\ell_{12}) & & & & \\ & & A^k(\ell_{23}) & & & \\ & & & \ddots & & \\ & & & & A^k(\ell_{(N-1)N}) & \\ & & & & & ik \end{pmatrix} \begin{pmatrix} f_1^- \\ f_1^+ \\ \vdots \\ f_N^- \\ f_N^+ \end{pmatrix}, \quad (2.7)$$

where for any real $\ell \in \mathbb{R}$, $A^k(\ell)$ denotes the 2×2 symmetric matrix

$$A^k(\ell) := \begin{pmatrix} -\frac{k \cos(k\ell)}{\sin(k\ell)} & \frac{k}{\sin(k\ell)} \\ \frac{k}{\sin(k\ell)} & -\frac{k \cos(k\ell)}{\sin(k\ell)} \end{pmatrix}. \quad (2.8)$$

Proof. Since from [\(2.4\)](#), $\frac{dw_f}{dx}(x) = ik(a_i e^{ikx} - b_i e^{-ikx})$ for $x \in (x_i^+, x_{i+1}^-)$, we can write

$$\begin{pmatrix} \frac{dw_f}{dx}(x_i^+) \\ -\frac{dw_f}{dx}(x_{i+1}^-) \end{pmatrix} = ik \begin{pmatrix} e^{ikx_i^+} & -e^{-ikx_i^+} \\ -e^{ikx_{i+1}^-} & e^{-ikx_{i+1}^-} \end{pmatrix} \begin{pmatrix} a_i \\ b_i \end{pmatrix}.$$

Replacing the constants a_i and b_i with the expression [\(2.3\)](#) yields

$$\begin{pmatrix} \mathcal{T}^k[f]_i^+ \\ \mathcal{T}^k[f]_{i+1}^- \end{pmatrix} = \begin{pmatrix} \frac{dw}{dx}(x_i^+) \\ -\frac{dw}{dx}(x_{i+1}^-) \end{pmatrix} = -\frac{k}{2\sin(k\ell_{i(i+1)})} \begin{pmatrix} e^{ikx_i^+} & -e^{-ikx_i^+} \\ -e^{ikx_{i+1}^-} & e^{-ikx_{i+1}^-} \end{pmatrix} \begin{pmatrix} e^{-ikx_{i+1}^-} & -e^{-ikx_i^+} \\ -e^{ikx_{i+1}^-} & e^{ikx_i^+} \end{pmatrix} \begin{pmatrix} f_i^+ \\ f_{i+1}^- \end{pmatrix}.$$

Computing the matrix product, we finally arrive at

$$\begin{pmatrix} \mathcal{T}^k[f]_i^+ \\ \mathcal{T}^k[f]_{i+1}^- \end{pmatrix} = A^k(\ell_{i(i+1)}) \begin{pmatrix} f_i^+ \\ f_{i+1}^- \end{pmatrix},$$

where $A^k(\ell_{i(i+1)})$ is the matrix defined by [\(2.8\)](#). Finally, since $w_f(x)$ is proportional to e^{ikx} when $x > x_N^+$ and to e^{-ikx} when $x < x_1^-$, we find $\mathcal{T}^k[f]_1^- = ikf_1^-$ and $\mathcal{T}^k[f]_N^+ = ikf_N^+$. \square

It can be verified that the solution w_f to [\(2.1\)](#) with $k \neq 0$ converges as $k \rightarrow 0$ to the solution to the same equation with $k = 0$. As it can be expected from the matrix representation [\(2.7\)](#), the operator \mathcal{T}^k is analytic in a neighborhood of $k = 0$. In all what follows, we denote by r the convergence radius

$$r := \frac{\pi}{\max_{1 \leq i \leq N-1} \ell_{i(i+1)}}.$$

The remaining part of this section is organized as follows. We remark in [Section 3.1](#) that the scattering problem (3.1) can be reformulated as a $2N \times 2N$ linear system, which gives a first characterization of the resonances and a computational methodology to solve numerically (3.1). However, this characterization is peculiar to the one-dimensional setting and does not lend itself to a convenient asymptotic analysis. In the next [Section 3.2](#), we use the formulation (3.1) to reduce the $2N \times 2N$ problem to a smaller $N \times N$ system involving a matrix $C(\omega, \delta)$ whose characteristic values ω are exactly the subwavelength resonances. In [Section 3.3](#), we relate the asymptotic expansions of the matrix $C(\omega, \delta)$ to the capacitance eigenvalue problem (1.9) with capacitance matrix (1.13). We deduce, in [Proposition 3.3](#), the existence of $2N$ subwavelength resonances and we compute explicitly their leading asymptotic expansion.

3.1. A first characterization of resonances based on an explicit representation of the solution

Let us first state a characterization of the resonances which relies on a finite dimensional parameterization of the solution u .

Lemma 3.1. *Any solution u to the wave problem (3.1) can be written as*

$$u(x) = a_i e^{ik_b x} + b_i e^{-ik_b x}, \quad \forall x \in (x_i^-, x_i^+),$$

for $2N$ coefficients $(a_i)_{1 \leq i \leq N}$ and $(b_i)_{1 \leq i \leq N}$ solutions to the $2N \times 2N$ linear system

$$\mathcal{A}(\omega, \delta) \begin{pmatrix} a_i \\ b_i \end{pmatrix}_{1 \leq i \leq N} = \begin{pmatrix} -\delta \mathcal{T}_v^\omega [u_{\text{in}}]_i^- - \delta \frac{du_{\text{in}}}{dx}(x_i^-) \\ -\delta \mathcal{T}_v^\omega [u_{\text{in}}]_i^+ + \delta \frac{du_{\text{in}}}{dx}(x_i^+) \end{pmatrix}_{1 \leq i \leq N}, \quad (3.3)$$

where $\mathcal{A}(\omega, \delta)$ is the $2N \times 2N$ matrix

$$\mathcal{A}(\omega, \delta) := ik_b \text{diag} \left(\begin{pmatrix} -e^{ik_b x_i^-} & e^{-ik_b x_i^-} \\ e^{ik_b x_i^+} & -e^{-ik_b x_i^+} \end{pmatrix} \right)_{1 \leq i \leq N} - \delta \mathcal{T}_v^\omega \times \text{diag} \left(\begin{pmatrix} e^{ik_b x_i^-} & e^{-ik_b x_i^-} \\ e^{ik_b x_i^+} & e^{-ik_b x_i^+} \end{pmatrix} \right)_{1 \leq i \leq N}, \quad (3.4)$$

and where \mathcal{T}_v^ω is the $2N \times 2N$ matrix defined by (2.7).

Proof. The boundary condition of (3.1) reads

$$\pm ik_b (a_i e^{ik_b x_i^\pm} - b_i e^{-ik_b x_i^\pm}) - \delta \mathcal{T}_v^\omega [u]_i^\pm = -\delta \mathcal{T}_v^\omega [u_{\text{in}}]_i^\pm \pm \delta \frac{du_{\text{in}}}{dx}(x_i^\pm),$$

which can be rewritten as (3.3). \square

Corollary 3.1. *Subwavelength resonances are complex frequencies $\omega(\delta)$ such that $\det(\mathcal{A}(\omega(\delta), \delta)) = 0$.*

Remark 3.1. The characterization (3.3) shows that the scattering problem (1.6) is a finite-dimensional problem that can be solved exactly by solving the $2N \times 2N$ linear system (3.3). We will exploit this formula in [Section 5](#) for solving (1.6) numerically.

3.2. Characterization of the resonances based on the Dirichlet-to-Neumann approach

Although (3.3) gives a complete characterization of the solution to (3.1), it does not allow to predict directly the arising of scattering resonances, since it seems rather tedious to compute asymptotic expansions of the determinant $\det(\mathcal{A}(\omega, \delta))$. In what follows, we use the Dirichlet-to-Neumann approach of [16, Section 3] to characterize the resonances very conveniently. This methodology exploits the physical structure of the system and applies to more complicated situations.

Multiplying by a test function $v \in H^1(D)$ and integrating on all the intervals (x_i^-, x_i^+) , equation (3.1) can be rewritten in the following weak form: find $u \in H^1(D)$ such that for any $v \in H^1(D)$,

$$a(u, v) = \langle f, v \rangle_{H^1(D), H^{-1}(D)}, \quad (3.5)$$

where a is the bilinear form on $H^1(D) \times H^1(D)$ defined by

$$a(u, v) := \sum_{i=1}^N \int_{x_i^-}^{x_i^+} \left(\frac{du}{dx} \frac{d\bar{v}}{dx} - \frac{\omega^2}{v_b^2} u \bar{v} \right) dx - \sum_{i=1}^N \delta \left[\bar{v}(x_i^+) \mathcal{T}_v^\omega [u]_i^+ + \bar{v}(x_i^-) \mathcal{T}_v^\omega [u]_i^- \right], \quad \forall u, v \in H^1(D),$$

and $f \in H^{-1}(D)$ is the linear form

$$\langle f, v \rangle_{H^1(D), H^{-1}(D)} := \delta \sum_{i=1}^N \left[\bar{v}(x_i^+) \left(-\mathcal{T}^k [u_{\text{in}}]_i^+ + \frac{du_{\text{in}}}{dx}(x_i^+) \right) + \bar{v}(x_i^-) \left(-\mathcal{T}^k [u_{\text{in}}]_i^- - \frac{du_{\text{in}}}{dx}(x_i^-) \right) \right]. \quad (3.6)$$

In what follows, we introduce a new bilinear form $a_{\omega,\delta}$ on $H^1(D)$:

$$a_{\omega,\delta}(u, v) := \sum_{i=1}^N \left[\int_{x_i^-}^{x_i^+} \frac{du}{dx} \frac{d\bar{v}}{dx} dx + \int_{x_i^-}^{x_i^+} u dx \int_{x_i^-}^{x_i^+} \bar{v} dx \right] - \sum_{i=1}^N \left[\frac{\omega^2}{v_b^2} \int_{x_i^-}^{x_i^+} u \bar{v} dx + \delta [\bar{v}(x_i^+) \mathcal{T}^k[u]_i^+ + \bar{v}(x_i^-) \mathcal{T}^k[u]_i^-] \right]. \quad (3.7)$$

The bilinear form $a_{\omega,\delta}(u, v)$ is obtained by adding the rank-one bilinear forms $(u, v) \rightarrow \int_{x_i^-}^{x_i^+} u dx \int_{x_i^-}^{x_i^+} \bar{v} dx$ to the bilinear form a . Clearly, $a_{\omega,\delta}$ is an analytic perturbation in ω and δ of the bilinear form $a_{0,0}$ defined by

$$a_{0,0}(u, v) = \sum_{i=1}^N \left[\int_{x_i^-}^{x_i^+} \frac{du}{dx} \frac{d\bar{v}}{dx} dx + \int_{x_i^-}^{x_i^+} u dx \int_{x_i^-}^{x_i^+} \bar{v} dx \right],$$

which is continuous coercive on $H^1(D)$ owing to the Poincaré-Wirtinger inequality. From standard perturbation theory, $a_{\omega,\delta}$ remains coercive for sufficiently small complex values of ω, δ . Therefore, for any right-hand-side $f \in H^{-1}(D)$, there exists a unique Lax-Milgram solution $u_f(\omega, \delta)$ to the problem

$$a_{\omega,\delta}(u_f(\omega, \delta), v) = \langle f, v \rangle_{H^{-1}(D), H^1(D)}, \quad (3.8)$$

which is analytic in ω and δ . In order to characterize resonant modes, we denote by $u_j(\omega, \delta)$ the solution to the variational problem

$$a_{\omega,\delta}(u_j(\omega, \delta), v) = \int_{x_j^-}^{x_j^+} \bar{v} dx, \quad \forall v \in H^1(D), \quad \forall 1 \leq j \leq N. \quad (3.9)$$

The functions $u_j(\omega, \delta)$ allow to reduce the $2N \times 2N$ problem (3.3) to a $N \times N$ matrix linear system, which is simpler to analyze.

Lemma 3.2. *Let $\omega \in \mathbb{C}$ and $\delta \in \mathbb{R}$ belong to a neighborhood of zero such that $a_{\omega,\delta}$ is coercive. For any right-hand side $f \in H^{-1}(D)$, the variational problem (3.5) admits a unique solution $u \equiv u(\omega, \delta)$ if and only if the $N \times N$ linear system*

$$(I - C(\omega, \delta))\mathbf{x} = \mathbf{F} \quad (3.10)$$

has a unique solution $\mathbf{x} := (x_i(\omega, \delta))_{1 \leq i \leq N}$, where $C(\omega, \delta)$ and \mathbf{F} are the matrix and column vector given by

$$C(\omega, \delta) \equiv (C(\omega, \delta)_{ij})_{1 \leq i, j \leq N} := \left(\int_{x_i^-}^{x_i^+} u_j(\omega, \delta) dx \right)_{1 \leq i, j \leq N}, \quad (3.11)$$

and

$$\mathbf{F} \equiv (F_i)_{1 \leq i \leq N} := \left(\int_{x_i^-}^{x_i^+} u_f(\omega, \delta) dx \right)_{1 \leq i \leq N}. \quad (3.12)$$

When it is the case, the solution to (3.5) (equivalently, to (1.6) and (3.1)) reads

$$u(\omega, \delta) = u_f(\omega, \delta) + \sum_{j=1}^N x_j(\omega, \delta) u_j(\omega, \delta), \quad (3.13)$$

with $u_f(\omega, \delta)$ and $u_j(\omega, \delta)$ being defined by (3.8) and (3.9).

When $I - C(\omega, \delta)$ is not invertible for a frequency $\omega \equiv \omega(\delta)$, then a linear combination of the functions $u_j(\omega, \delta)$ is a nonzero solution to (3.5), and ω is a subwavelength resonance.

Proof. The variational problem (3.5) reads equivalently

$$\begin{aligned} a(u, v) = \langle f, v \rangle_{H^{-1}(D), H^1(D)} &\Leftrightarrow a_{\omega,\delta}(u, v) - \sum_{i=1}^N \left(\int_{x_i^-}^{x_i^+} u dx \right) a_{\omega,\delta}(u_i, v) = a_{\omega,\delta}(u_f(\omega, \delta), v) \\ &\Leftrightarrow u - \sum_{i=1}^N \left(\int_{x_i^-}^{x_i^+} u dx \right) u_i = u_f(\omega, \delta). \end{aligned} \quad (3.14)$$

By integrating both sides of (3.14) on (x_i^-, x_i^+) , we find that the vector $\mathbf{x} := \left(\int_{x_i^-}^{x_i^+} u(\omega, \delta) dx \right)_{1 \leq i \leq N}$ solves the linear system

$$\int_{x_i^-}^{x_i^+} u(\omega, \delta) dx - \sum_{j=1}^N \int_{x_i^-}^{x_i^+} u_j(\omega, \delta) dx \int_{x_j^-}^{x_j^+} u(\omega, \delta) dx = \int_{x_i^-}^{x_i^+} u_f(\omega, \delta) dx, \quad 1 \leq i \leq N,$$

which is exactly (3.10). Reciprocally, if (3.10) has a solution, then the second line of (3.14) shows that the solution to (3.5) is given by (3.13). \square

Subwavelength resonances are therefore the characteristic values $\omega \equiv \omega(\delta)$ for which $I - C(\omega, \delta)$ is not invertible. Furthermore, (3.13) yields a modal decomposition of the solution when ω is not a resonant frequency.

3.3. Asymptotic expansions of the subwavelength resonances

We now show the existence of $2N$ subwavelength resonances and we compute their leading-order asymptotic expansions. We start by computing explicit asymptotic expansions of the functions $u_i(\omega, \delta)$ solutions to (3.9). Here and thereafter, the characteristic function of the interval (x_i^-, x_i^+) is written $1_{(x_i^-, x_i^+)}$:

$$1_{(x_i^-, x_i^+)}(t) = \begin{cases} 1 & \text{if } t \in (x_i^-, x_i^+), \\ 0 & \text{otherwise.} \end{cases}$$

Proposition 3.1. *Let $\omega \in \mathbb{C}$ and $\delta \in \mathbb{R}$ belong to a neighborhood of zero. The unique solution $u_j(\omega, \delta)$ with $1 \leq j \leq N$ to the variational problem (3.9) has the following asymptotic behavior as $\omega, \delta \rightarrow 0$:*

$$\begin{aligned} u_j(\omega, \delta) &= \left(\frac{1}{\ell_j} + \frac{\omega^2}{v_b^2 \ell_j^2} \right) 1_{(x_j^-, x_j^+)} \\ &+ \delta \left[\frac{1}{\ell_{j-1}^2 \ell_j} \frac{1}{\ell_{(j-1)j}} 1_{(x_{j-1}^-, x_{j-1}^+)} - \frac{1}{\ell_j^3} \left(\frac{1}{\ell_{(j-1)j}} + \frac{1}{\ell_{j(j+1)}} \right) 1_{(x_j^-, x_j^+)} + \frac{1}{\ell_j \ell_{j+1}^2} \frac{1}{\ell_{j(j+1)}} 1_{(x_{j+1}^-, x_{j+1}^+)} + \tilde{u}_{j,0,1} \right] \\ &+ \frac{i\omega\delta}{\ell_j^3 v} (\delta_{j1} + \delta_{jN}) \left(1_{(x_j^-, x_j^+)} + \tilde{u}_{j,1,1} \right) + O((\omega^2 + \delta)^2), \end{aligned} \quad (3.15)$$

where $\tilde{u}_{j,0,1}$ and $\tilde{u}_{j,1,1}$ are some (quadratic) functions satisfying

$$\int_{x_i^-}^{x_i^+} \tilde{u}_{j,0,1} dx = 0, \quad \int_{x_i^-}^{x_i^+} \tilde{u}_{j,1,1} dx = 0, \quad \forall 1 \leq i \leq N.$$

Proof. From the definition of $a_{\omega, \delta}$, the function $u_j \equiv u_j(\omega, \delta)$ satisfies the following differential equation written in strong form:

$$\begin{cases} -\frac{d^2}{dx^2} u_j - \frac{\omega^2}{v_b^2} u_j + \sum_{i=1}^N \left(\int_{x_i^-}^{x_i^+} u_j dx \right) 1_{(x_i^-, x_i^+)} = 1_{(x_j^-, x_j^+)} & \text{in } \bigsqcup_{i=1}^N (x_i^-, x_i^+), \\ \pm \frac{du_j}{dx} (x_i^\pm) = \delta \mathcal{T}^{\frac{\omega}{v}} [u_j]_i^\pm & \text{for all } 1 \leq i \leq N. \end{cases} \quad (3.16)$$

Since $u_j(\omega, \delta)$ is analytic in ω and δ , there exist functions $(u_{j,p,k})_{p \geq 0, k \geq 0}$ such that $u_j(\omega, \delta)$ can be written as the following convergent series in $H^1(D)$:

$$u_j(\omega, \delta) = \sum_{p,k=0}^{+\infty} \omega^p \delta^k u_{j,p,k}. \quad (3.17)$$

By using Corollary 2.1 and identifying powers of ω and δ , we obtain the following equations characterizing the functions $(u_{j,p,k})_{p \geq 0, k \geq 0}$:

$$\begin{cases} -\frac{d^2}{dx^2} u_{j,p,k} + \sum_{i=1}^N \left(\int_{x_i^-}^{x_i^+} u_{j,p,k} dx \right) 1_{(x_i^-, x_i^+)} = \frac{1}{v_b^2} u_{j,p-2,k} + 1_{(x_j^-, x_j^+)} \delta_{p=0} \delta_{k=0} & \text{in } \bigsqcup_{i=1}^N (x_i^-, x_i^+), \\ \pm \frac{du_{j,p,k}}{dx} (x_i^\pm) = \sum_{n=0}^p \frac{1}{v^n} \mathcal{T}_n [u_{j,p-n,k-1}]_i^\pm & \text{for all } 1 \leq i \leq N, \end{cases}$$

with the convention that $u_{j,p,k} = 0$ for negative indices p and k . It can then be easily obtained by induction that

$$u_{j,2p,0} = \frac{1_{(x_j^-, x_j^+)}}{v_b^{2p} \ell_j^{p+1}} \text{ and } u_{j,2p+1,0} = 0, \text{ for any } p \geq 0.$$

Then for $p = 0$ and $k = 1$, we find that $u_{j,0,1}$ satisfies

$$\begin{cases} -\frac{d^2}{dx^2} u_{j,0,1} + \sum_{i=1}^N \left(\int_{x_i^-}^{x_i^+} u_{j,0,1} dx \right) 1_{(x_i^-, x_i^+)} = 0 & \text{in } \bigsqcup_{i=1}^N (x_i^-, x_i^+), \\ \pm \frac{du_{j,0,1}}{dx} (x_i^\pm) = \mathcal{T}_0 [u_{j,0,0}]_i^\pm & \text{for all } 1 \leq i \leq N. \end{cases} \quad (3.18)$$

From (2.11) with $f_i^\pm := u_{j,0,0}(x_i^\pm) = \delta_{ij}/\ell_j$, we obtain

$$\begin{cases} \mathcal{T}_0[u_{j,0,0}]_1^- = 0, \\ \mathcal{T}_0[u_{j,0,0}]_i^- = -\frac{1}{\ell_j} \frac{1}{\ell_{(i-1)j}} (\delta_{ij} - \delta_{(i-1)j}) & \text{for } 2 \leq i \leq N, \\ \mathcal{T}_0[u_{j,0,0}]_i^+ = \frac{1}{\ell_j} \frac{1}{\ell_{i(i+1)}} (\delta_{(i+1)j} - \delta_{ij}) & \text{for } 1 \leq i \leq N-1, \\ \mathcal{T}_0[u_{j,0,0}]_N^+ = 0. \end{cases}$$

Multiplying (3.18) by $1_{(x_i^-, x_i^+)}$ and integrating by parts, we find that

$$\begin{aligned} \int_{x_i^-}^{x_i^+} u_{j,0,1} dx &= \frac{1}{\ell_i} [\mathcal{T}_0[u_{j,0,0}]_i^- + \mathcal{T}_0[u_{j,0,0}]_i^+] \\ &= \frac{1}{\ell_i \ell_j} \frac{1}{\ell_{(j-1)i}} (\delta_{(i-1)j} - \delta_{ij}) \mathbf{1}_{2 \leq j \leq N} + \frac{1}{\ell_i \ell_j} \frac{1}{\ell_{i(i+1)}} (\delta_{(i+1)j} - \delta_{ij}) \mathbf{1}_{1 \leq j \leq N-1} \\ &= \begin{cases} \frac{1}{\ell_{j-1} \ell_j} \frac{1}{\ell_{(j-1)j}} & \text{if } i = j-1, \\ -\frac{1}{\ell_j^2} \left(\frac{1}{\ell_{(j-1)j}} + \frac{1}{\ell_{j(j+1)}} \right) & \text{if } i = j, \\ \frac{1}{\ell_j \ell_{j+1}} \frac{1}{\ell_{j(j+1)}} & \text{if } i = j+1. \end{cases} \end{aligned}$$

Using Fredholm's alternative, this allows to infer that $u_{j,0,1}$ can be written as

$$u_{j,0,1} = \frac{1}{\ell_{j-1}^2 \ell_j} \frac{1}{\ell_{(j-1)j}} \mathbf{1}_{(x_{j-1}^-, x_{j-1}^+)} - \frac{1}{\ell_j^3} \left(\frac{1}{\ell_{(j-1)j}} + \frac{1}{\ell_{j(j+1)}} \right) \mathbf{1}_{(x_j^-, x_j^+)} + \frac{1}{\ell_j \ell_{j+1}^2} \frac{1}{\ell_{j(j+1)}} \mathbf{1}_{(x_{j+1}^-, x_{j+1}^+)} + \tilde{u}_{j,0,1},$$

where $\tilde{u}_{j,0,1}$ is a function (in fact, a second order polynomial) satisfying $\int_{x_i^-}^{x_i^+} \tilde{u}_{j,0,1} dx = 0$ for any $1 \leq i \leq N$.

Furthermore, $\tilde{u}_{j,0,1}$ is identically zero on (x_i^-, x_i^+) where $i \notin \{j-1, j, j+1\}$.

Finally, let us compute $u_{j,1,1}$, which satisfies

$$\begin{cases} -\frac{d^2}{dx^2} u_{j,1,1} + \sum_{i=1}^N \left(\int_{x_i^-}^{x_i^+} u_{j,1,1} dx \right) \mathbf{1}_{(x_i^-, x_i^+)} = 0 & \text{in } \bigsqcup_{i=1}^N (x_i^-, x_i^+), \\ \pm \frac{du_{j,1,1}}{dx}(x_i^\pm) = \frac{1}{v} \mathcal{T}_1[u_{j,0,0}]_i^\pm & \text{for all } 1 \leq i \leq N. \end{cases} \quad (3.19)$$

Similarly, we find that $\mathcal{T}_1[u_{j,0,0}]_i^\pm$ is given by

$$\mathcal{T}_1[u_{j,0,0}]_i^- = \begin{cases} \frac{i}{\ell_j} \delta_{j1} & \text{if } i = 1, \\ 0 & \text{if } i \geq 2, \end{cases} \quad \mathcal{T}_1[u_{j,0,0}]_i^+ = \begin{cases} 0 & \text{if } i \leq N-1, \\ \frac{i}{\ell_j} \delta_{jN} & \text{if } i = N. \end{cases}$$

Consequently, multiplying (3.19) by $1_{(x_i^-, x_i^+)}$ and integrating by parts yields

$$\int_{x_i^-}^{x_i^+} u_{j,1,1} dx = \frac{i}{\ell_i \ell_j v} (\delta_{i1} \delta_{j1} + \delta_{iN} \delta_{jN}).$$

This implies that $u_{j,1,1} = \frac{i}{\ell_j^3 v} (\delta_{j1} + \delta_{jN}) \mathbf{1}_{(x_j^-, x_j^+)} + \tilde{u}_{j,1,1}$, where $\tilde{u}_{j,1,1}$ is a function satisfying $\int_{x_i^-}^{x_i^+} \tilde{u}_{j,1,1} dx = 0$ for any $1 \leq i \leq N$. The result follows. \square

In what follows, we recall the definitions (1.12) and (1.13) of the $N \times N$ tridiagonal capacitance matrix C , and the definition (1.14) of the volume matrix V . We also introduce the $N \times N$ matrix

$$B = \text{diag}(1, 0, \dots, 0, 1). \quad (3.20)$$

These matrices C , V and B arise in the asymptotic expansion of $C(\omega, \delta)$ of (3.11).

Corollary 3.2. *We have the following asymptotic expansion for the matrix $C(\omega, \delta)$ defined in (3.11):*

$$C(\omega, \delta) = I + \frac{\omega^2}{v_b^2} V^{-1} - \delta V^{-1} C V^{-1} + \frac{i\omega\delta}{v} V^{-1} B V^{-1} + O((\omega^2 + \delta)^2), \quad (3.21)$$

where C is the ‘‘capacitance matrix’’ of (1.13), and B and V are the matrices of (3.20).

Proof. Integrating the asymptotic expansion (3.15) of $u_j(\omega, \delta)$ on the interval (x_i^-, x_i^+) , we obtain

$$C_{ij}(\omega, \delta) = \left(1 + \frac{\omega^2}{v_b^2 \ell_i}\right) \delta_{ij} + \delta \left[\frac{1}{\ell_i \ell_j} \frac{1}{\ell_{(j-1)j}} \delta_{i(j-1)} - \frac{1}{\ell_i \ell_j} \left(\frac{1}{\ell_{(j-1)j}} + \frac{1}{\ell_{j(j+1)}} \right) \delta_{ij} + \frac{1}{\ell_i \ell_j} \frac{1}{\ell_{j(j+1)}} \delta_{i(j+1)} \right] + \frac{i\omega\delta}{\ell_j^2 v} \delta_{ij} (\delta_{j1} + \delta_{jN}) + O((\omega^2 + \delta)^2).$$

This yields the result. \square

The next proposition shows that C is a nonnegative symmetric matrix.

Proposition 3.2. *The capacitance matrix of (1.13) is a symmetric positive semi-definite matrix. Furthermore, the null space of C is the one-dimensional vector space spanned by the vector of ones:*

$$\text{Ker } C = \text{span}(\mathbf{1}) \text{ where } \mathbf{1} := (1)_{1 \leq i \leq N}.$$

Proof. For a real vector $\mathbf{f} = (f_i)_{1 \leq i \leq N}$, and using the conventions $f_{-1} = f_{N+1} = 0$ and $1/\ell_{i(i+1)} = 0$ for $i = -1, N$, we easily compute

$$\begin{aligned} \mathbf{f}^T C \mathbf{f} &= \sum_{i=1}^N \left[-\frac{1}{\ell_{(i-1)i}} f_{i-1} f_i + \left(\frac{1}{\ell_{(i-1)i}} + \frac{1}{\ell_{i(i+1)}} \right) f_i^2 - \frac{1}{\ell_{i(i+1)}} f_i f_{i+1} \right] \\ &= \sum_{i=1}^{N-1} \left[-\frac{1}{\ell_{i(i+1)}} f_i f_{i+1} + \frac{1}{\ell_{i(i+1)}} f_{i+1}^2 + \frac{1}{\ell_{i(i+1)}} f_i^2 - \frac{1}{\ell_{i(i+1)}} f_i f_{i+1} \right] \\ &= \sum_{i=1}^{N-1} \frac{1}{\ell_{i(i+1)}} (f_{i+1} - f_i)^2. \end{aligned}$$

Since $\ell_{i(i+1)} > 0$ for any $1 \leq i \leq N-1$, this equality shows that $\mathbf{f}^T C \mathbf{f} \geq 0$ for any $\mathbf{f} \in \mathbb{R}^N$, which implies that C is nonnegative. Furthermore, $\mathbf{f}^T C \mathbf{f} = 0$ implies $f_{i+1} = f_i$ for any $1 \leq i \leq N-1$, which means that \mathbf{f} is proportional to the vector of ones. \square

Remark 3.2. In three-dimensions, special properties arise when the vector of ones is an eigenvector of the capacitance matrix, which is the case under special symmetry circumstances [15, Section 2]. The result of Proposition 3.2 shows that $\mathbf{1}$ is always an eigenvector of the capacitance matrix in the 1D situation, which is associated to the zero eigenvalue. We shall see in Proposition 3.3 that this physically corresponds to the fact that in 1D, constant functions are resonant modes. Non-trivial eigenvalues arise therefore for a system of at least $N = 2$ resonators.

Next, we consider the N eigenvalues $(\lambda_i)_{1 \leq i \leq N}$ and eigenvectors $(\mathbf{a}_i)_{1 \leq i \leq N}$ of the generalized eigenvalue problem (1.9):

$$C \mathbf{a}_i = \lambda_i V \mathbf{a}_i, \quad 1 \leq i \leq N, \quad (3.22)$$

where the eigenvectors form an orthonormal basis with respect to the inner product of V :

$$\mathbf{a}_i^T V \mathbf{a}_j = \delta_{ij}, \quad \forall 1 \leq i, j \leq N,$$

and the vector \mathbf{a}_1 is given by

$$\mathbf{a}_1 = \frac{1}{\sqrt{\sum_{i=1}^N \ell_i}} \mathbf{1}.$$

The tridiagonal structure of C implies the simplicity of the eigenvalues:

Lemma 3.3. *The N eigenvalues of the capacitance matrix C are simple:*

$$0 = \lambda_1 < \lambda_2 < \dots < \lambda_N.$$

Proof. This results from the fact that C is a tridiagonal matrix with non-zero off-diagonal elements, see [31, Lemma 7.7.1]. \square

The next corollary shows the arising of exactly $2N$ resonant frequencies whose leading order asymptotics are related to the eigenvalues $(\lambda_i)_{1 \leq i \leq N}$.

Proposition 3.3. *The scattering problem (1.6) admits exactly $2N$ resonant frequencies:*

- the zero frequency $\omega_0(\delta) = 0$ for any $\delta > 0$,
- a purely imaginary frequency $\omega_1(\delta)$, which is an analytic function of δ whose leading asymptotic expansion reads:

$$\omega_1(\delta) = -2i\delta \frac{v_b^2}{v \sum_{j=1}^N \ell_j} + O(\delta^2); \quad (3.23)$$

- the remaining $2N-2$ resonant frequencies are analytic functions of $\delta^{\frac{1}{2}}$ and their leading-order asymptotic expansion read

$$\omega_i^\pm(\delta) = \pm v_b \lambda_i^{\frac{1}{2}} \delta^{\frac{1}{2}} - i\delta \frac{v_b^2}{2v} \mathbf{a}_i^T B \mathbf{a}_i + O(\delta^{\frac{3}{2}}) \text{ for } 2 \leq i \leq N, \quad (3.24)$$

where B is the matrix defined in (3.20).

Proof. We proceed as in the proof of [15, Propositions 3.7 and 3.9]. We pose $\lambda := \frac{\omega^2}{\delta}$ and introduce the function

$$F((\lambda, \mathbf{x}), \omega) := \left(\frac{\lambda}{\omega^2} \left(I - C \left(\omega, \frac{\omega^2}{\lambda} \right) \right) V \mathbf{x}, \mathbf{x}^T V \mathbf{x} - 1 \right).$$

First, we observe that F is a smooth function of $\omega \in \mathbb{C}$ and $\lambda \in \mathbb{C}$ because

$$\frac{\lambda}{\omega^2} \left(I - C \left(\omega, \frac{\omega^2}{\lambda} \right) \right) V \mathbf{x} = \left(-\frac{\lambda}{v_b^2} I + V^{-1} C - \frac{i\omega}{v} V^{-1} B + O(\omega^2) \right) \mathbf{x}.$$

Then for $\omega = 0$, it holds $F((\lambda_i v_b^2, \mathbf{a}_i), 0) = 0$. Applying the implicit function theorem as in [15, Proposition 3.7] (this is possible thanks to the simplicity result of Lemma 3.3), we obtain the existence of analytic functions $\lambda_i(\omega)$ and $\mathbf{a}_i(\omega)$ satisfying

$$F((\lambda_i(\omega), \mathbf{a}_i(\omega)), \omega) = 0 \quad (3.25)$$

with $\lambda_i(0) = \lambda_i v_b^2$ and $\mathbf{a}_i(0) = \mathbf{a}_i$, for $\omega \in \mathbb{C}$ belonging to a neighborhood of zero. Furthermore, differentiating (3.25) with respect to ω at $\omega = 0$, we find that $\lambda'_i(0)$ and $\mathbf{a}'_i(0)$ satisfy

$$-\frac{\lambda'_i(0)}{v_b^2} \mathbf{a}_i - \frac{i}{v} V^{-1} B \mathbf{a}_i + \left(-\frac{\lambda_i}{v_b^2} I + V^{-1} C \right) \mathbf{a}'_i(0) = 0.$$

Left multiplying by $\mathbf{a}_i^T V$ and using $\mathbf{a}'_i(0)^T V \mathbf{a}_i = 0$, we obtain

$$\lambda'_i(0) = -\frac{i v_b^2}{v} \mathbf{a}_i^T B \mathbf{a}_i, \quad \mathbf{a}'_i(0) = \frac{i}{v} \sum_{j \neq i} \frac{\mathbf{a}_j^T B \mathbf{a}_i}{(\lambda_j - \lambda_i)} \mathbf{a}_j,$$

which allows to infer that

$$\lambda_i(\omega) = \lambda_i v_b^2 - \frac{i \omega v_b^2}{v} \mathbf{a}_i^T B \mathbf{a}_i + O(\omega^2), \quad (3.26)$$

and

$$\mathbf{a}_i(\omega) = \mathbf{a}_i + \frac{i \omega}{v} \sum_{j \neq i} \frac{\mathbf{a}_j^T B \mathbf{a}_i}{v(\lambda_j - \lambda_i)} \mathbf{a}_j + O(\omega^2). \quad (3.27)$$

Subwavelength resonant frequencies ω are the solutions to the equation $\omega^2 = \delta \lambda_i(\omega)$. For $i = 1$, we obtain the equation

$$\omega^2 = \delta \left(-\frac{i \omega v_b^2}{v} \mathbf{a}_1^T B \mathbf{a}_1 + O(\omega^2) \right).$$

This yields the zero frequency $\omega = 0$, or

$$\omega = \delta \left(-\frac{i v_b^2}{v} \mathbf{a}_1^T B \mathbf{a}_1 + O(\omega) \right),$$

which admits a solution $\omega_1(\delta)$ analytic in δ satisfying

$$\omega_1(\delta) = -i\delta \frac{v_b^2}{v} \mathbf{a}_1^T B \mathbf{a}_1 + O(\delta^2) = -i\delta \frac{v_b^2}{v} \frac{2}{\sum_{i=1}^N \ell_i} + O(\delta^2),$$

i.e. (3.2).

For $2 \leq i \leq N$, $\lambda_i \neq 0$ and the equation $\omega^2 = \delta \lambda_i(\omega)$ is then equivalent to

$$\omega = \delta^{\frac{1}{2}} \sqrt{\lambda_i(\omega)} \text{ or } \omega = -\delta^{\frac{1}{2}} \sqrt{\lambda_i(\omega)},$$

where $\sqrt{\cdot}$ denotes any analytic continuation of the square root on $\mathbb{C} \setminus \{it \mid t < 0\}$. Solving these equations with the implicit function theorem yields two resonant frequencies $\omega_i^\pm(\delta)$ which are analytic in $\delta^{\frac{1}{2}}$. Using (3.26), we obtain $\omega_i^\pm(\delta) \sim \delta^{\frac{1}{2}} v_b \lambda_i^{\frac{1}{2}}$, and the next order term can be retrieved by writing

$$\begin{aligned} \omega_i^\pm(\delta) &= \pm \delta^{\frac{1}{2}} \lambda_i^{\frac{1}{2}} v_b \sqrt{1 \mp \frac{i \delta^{\frac{1}{2}} \lambda_i^{\frac{1}{2}} v_b}{v \lambda_i} \mathbf{a}_i^T B \mathbf{a}_i + O(\delta)} = \pm \delta^{\frac{1}{2}} \lambda_i^{\frac{1}{2}} v_b \left(1 \mp \frac{i \delta^{\frac{1}{2}} \lambda_i^{-\frac{1}{2}} v_b}{2v} \mathbf{a}_i^T B \mathbf{a}_i + O(\delta) \right) \\ &= \pm \delta^{\frac{1}{2}} \lambda_i^{\frac{1}{2}} v_b - i\delta \frac{v_b^2}{2v} \mathbf{a}_i^T B \mathbf{a}_i + O(\delta^{\frac{3}{2}}), \end{aligned}$$

which yields (3.24).

It remains to show that $\omega_1(\delta)$ is a purely imaginary complex number. From Corollary 2.1, the Dirichlet-to-Neumann map \mathcal{T}^k satisfies $\overline{\mathcal{T}^k} = \mathcal{T}^{-k}$. From (3.2), we deduce that if ω is a resonant frequency with resonant

mode $v(\omega, \delta)$, then $-\bar{\omega}$ must also be a resonant frequency with resonant mode $\overline{v(\omega, \delta)}$. Therefore, $-\overline{\omega_1(\delta)}$ must also be a resonant frequency. From the Rouché general argument principle, the nonlinear eigenvalue $\omega = 0$ at $\delta = 0$ has algebraic multiplicity $2N$. Hence, it must split in exactly $2N$ branches as δ deviates from zero. Consequently, $-\overline{\omega_1(\delta)}$ and $\omega_1(\delta)$ must coincide, which is possible only if $\omega_1(\delta)$ is purely imaginary. \square

Remark 3.3. The resonant mode associated to the zero frequency $\omega_0(\delta) = 0$ is the constant mode $u = 1$ in \mathbb{R} . The occurrence of this mode, absent in the 3D setting, is due to the fact that there is no function satisfying $-\mathrm{d}^2u/\mathrm{d}x^2 = 0$, $u(x_1^-) = u(x_N^+) = 1$ and decaying at infinity. The mode associated to the purely imaginary frequency $\omega_1(\delta)$ is approximately constant in each segment $(x_i^-, x_i^+)_{1 \leq i \leq N}$ and grows exponentially as $|x| \rightarrow +\infty$, but decays exponentially in time. These phenomena are illustrated on [Figure 6](#) in the numerical section below.

Remark 3.4. It is possible to compute $w_1(\delta)$ explicitly in the single resonator case $N = 1$. Computing the roots of the determinant of the matrix $\mathcal{A}(\omega, \delta)$ of [\(3.4\)](#), we find the exact formula

$$w_1(\delta) = -iv_b \log \left(1 + \frac{2v_b\delta}{v - v_b\delta} \right). \quad (3.28)$$

4. MODAL DECOMPOSITIONS AND TRANSMISSION PROPERTIES IN THE HIGH-CONTRAST MEDIUM

In this section, we compute a modal decomposition for the wave solution based on the representation [\(3.13\)](#), and study transmission properties of incident waves through the high-contrast medium.

The modal decomposition of the total wave field is established in [Section 4.1](#). We obtain that in the subwavelength regime, the solution to the non-hermitian scattering problem [\(1.6\)](#) can be approximated as a superposition of modes which are excited near the resonant frequencies. Then, [Section 4.2](#) introduces the transmission and reflection coefficients, which capture the effective scattering properties of the high-contrast system of resonators. We obtain approximate formulas in the subwavelength regime ([Proposition 4.5](#)), and we establish the identities [\(1.16\)](#) for the values of the transmission and reflection coefficients taken to the resonant frequencies.

4.1. Modal decomposition of the wave total field

A modal decomposition of the total wave field can be obtained from the characterization [\(3.13\)](#) of the solution. In this part, we assume that the incident field u_{in} solution to [\(1.4\)](#) can be written as

$$u_{\text{in}}(x) = \alpha_+ e^{ikx} + \alpha_- e^{-ikx}, \quad (4.1)$$

where α_+ and α_- are two constants chosen independently of ω and δ . The wave u_{in} is therefore the superposition of the wave $\alpha_+ e^{ikx}$ travelling from left to right, and of the wave $\alpha_- e^{-ikx}$ propagating in the opposite direction.

We first need an asymptotic expansion of the solution $u_f(\omega, \delta)$ to the variational problem [\(3.8\)](#).

Proposition 4.1. *Let f be the right-hand side [\(3.6\)](#). The function $u_f(\omega, \delta)$ solution to [\(3.8\)](#) has the following first order asymptotic expansion:*

$$u_f(\omega, \delta)(x) = -\frac{2i\omega\delta}{v} \left(\frac{\alpha_+}{\ell_1^2} \mathbf{1}_{(x_1^-, x_1^+)} + \frac{\alpha_-}{\ell_N^2} \mathbf{1}_{(x_N^-, x_N^+)} + \tilde{v}_{1,1}(x) \right) + O(\omega^2\delta), \quad (4.2)$$

where $\tilde{v}_{1,1}$ is a (quadratic) function vanishing on (x_i^-, x_i^+) for $2 \leq i \leq N-1$ and satisfying $\int_{x_i^-}^{x_i^+} \tilde{v}_{1,1} dx = 0$ for $i = 1$ or $i = N$.

Proof. The variational problem [\(3.8\)](#) reads in strong form

$$\begin{cases} -\frac{\mathrm{d}^2}{\mathrm{d}x^2} u_f - \frac{\omega^2}{v_b^2} u_f + \sum_{i=1}^N \left(\int_{x_i^-}^{x_i^+} u_f dx \right) \mathbf{1}_{(x_i^-, x_i^+)} = 0 & \text{in } \bigsqcup_{i=1}^N (x_i^-, x_i^+), \\ \pm \frac{\mathrm{d}u_f}{\mathrm{d}x}(x_i^\pm) - \delta \mathcal{T}^{\frac{\omega}{v}} [u_f]_i^\pm = -\delta \mathcal{T}^{\frac{\omega}{v}} [u_{\text{in}}]_i^\pm \pm \delta \frac{\mathrm{d}u_{\text{in}}}{\mathrm{d}x}(x_i^\pm) & \text{for all } 1 \leq i \leq N. \end{cases} \quad (4.3)$$

From [\(4.1\)](#), u_{in} can be approximated by the following asymptotic development inside the resonators:

$$u_{\text{in}}(x) = \alpha_+ + \alpha_- + \frac{i\omega}{v} (\alpha_+ - \alpha_-) x + O(\omega^2), \quad x \in \bigsqcup_{i=1}^N (x_i^-, x_i^+).$$

This yields the following asymptotic expansion for the right-hand side of [\(4.3\)](#):

$$\begin{aligned} -\delta \mathcal{T}^{\frac{\omega}{v}} [u_{\text{in}}]_i^\pm \pm \delta \frac{\mathrm{d}u_{\text{in}}}{\mathrm{d}x}(x_i^\pm) &= \delta \left(-\left(\mathcal{T}^0 + \frac{\omega}{v} \mathcal{T}^1 \right) \left[\alpha_+ + \alpha_- + \frac{i\omega}{v} (\alpha_+ - \alpha_-) x \right]_i^\pm \pm \frac{i\omega}{v} (\alpha_+ - \alpha_-) + O(\omega^2) \right) \\ &= \delta \left(-(\alpha_+ - \alpha_-) \frac{i\omega}{v} \mathcal{T}_0[x]_i^\pm - \frac{i\omega}{v} (\alpha_+ + \alpha_-) (\delta_{i1}^- + \delta_{iN}^+) \pm \frac{i\omega}{v} (\alpha_+ - \alpha_-) + O(\omega^2) \right). \end{aligned}$$

Since $u_f(\omega, \delta)$ is analytic in ω and δ and the right-hand side is of order $O(\omega\delta)$, we can write the ansatz

$$u_f(\omega, \delta) = \omega\delta v_{1,1} + O(\omega^2\delta).$$

Inserting this expression into (4.3), we obtain the following equation for $v_{1,1}$:

$$\left\{ \begin{array}{l} -\frac{d^2}{dx^2}v_{1,1} + \sum_{i=1}^N \left(\int_{x_i^-}^{x_i^+} v_{1,1} dx \right) \mathbf{1}_{(x_i^-, x_i^+)} = 0 \\ \pm \frac{dv_{1,1}}{dx}(x_i^\pm) = -\frac{i}{v} \left((\alpha_+ - \alpha_-) \mathcal{T}_0[x]_i^\pm \right. \\ \left. + (\alpha_+ + \alpha_-)(\delta_{i1}^- + \delta_{iN}^+) \mp (\alpha_+ - \alpha_-) \right) \end{array} \right. \quad \text{in } \prod_{i=1}^N (x_i^-, x_i^+), \quad \text{for all } 1 \leq i \leq N. \quad (4.4)$$

Integrating by parts on (x_i^-, x_i^+) and using (2.11), we infer

$$\begin{aligned} \int_{x_i}^{x_i^+} v_{1,1} dx &= -\frac{i}{\ell_i v} \left((\alpha_+ - \alpha_-) [\mathcal{T}_0[x]_i^- + \mathcal{T}_0[x]_i^+] + (\alpha_+ + \alpha_-)(\delta_{i1} + \delta_{iN}) \right) \\ &= -\frac{i}{\ell_i v} \left((\alpha_+ - \alpha_-) \left(-\frac{x_i^- - x_{i-1}^+}{\ell_{(i-1)i}} \delta_{2 \leq i \leq N} + \frac{x_{i+1}^- - x_i^+}{\ell_{i(i+1)}} \delta_{1 \leq i \leq N-1} \right) + (\alpha_+ + \alpha_-)(\delta_{i1} + \delta_{iN}) \right) \\ &= -\frac{2i}{\ell_i v} [\alpha_+ \delta_{i1} + \alpha_- \delta_{iN}]. \end{aligned}$$

From the Fredholm alternative, we deduce that the function $v_{1,1}$ is given by

$$v_{1,1} = -\frac{2i}{v} \left[\frac{\alpha_+}{\ell_1^2} \mathbf{1}_{(x_1^-, x_1^+)} + \frac{\alpha_-}{\ell_N^2} \mathbf{1}_{(x_N^-, x_N^+)} + \tilde{v}_{1,1}(x) \right],$$

where $\tilde{v}_{1,1}$ is a function vanishing on (x_i^-, x_i^+) for $2 \leq i \leq N-1$ and satisfying $\int_{x_i^-}^{x_i^+} \tilde{v}_{1,1} dx = 0$ for $i = 1$ or $i = N$. This yields the result. \square

Remark 4.1. The expansion of (4.2) shows that an incident wave e^{ikx} (resp. e^{-ikx}) propagating from left to right (resp. from right to left) excites only the first resonator (x_1^-, x_1^+) (resp. the last resonator (x_N^-, x_N^+)) at first order.

Proposition 4.2. *Assume that ω is real and belongs to the subwavelength regime $\omega = O(\delta^{\frac{1}{2}})$. For any right-hand side $\mathbf{F} \in \mathbb{C}^N$, the solution $\mathbf{x}(\omega, \delta)$ to (3.10) can be decomposed as the following modal decomposition:*

$$\mathbf{x}(\omega, \delta) = -\sum_{j=1}^N \frac{v_b^2}{\omega^2 - \delta v_b^2 \lambda_j + i\omega \delta \frac{v_b^2}{v} \mathbf{a}_j^T B \mathbf{a}_j} (1 + O(\delta^{\frac{1}{2}})) (\mathbf{a}_j^T V \mathbf{F}) V \mathbf{a}_j. \quad (4.5)$$

Proof. In order to solve (3.10), we use the same notation as the ones of the proof of Proposition 3.3, and proceed as in the proofs of [15, Propositions 3.9, 3.10 and 4.1]. Introducing $\lambda := \frac{\omega^2}{\delta}$, $\mathbf{y} := V^{-1} \mathbf{x}$, $\mathcal{G}(\omega, \lambda) := \frac{\lambda}{\omega^2} \left(I - C \left(\omega, \frac{\omega^2}{\lambda} \right) \right) V$ and $\hat{\mathbf{F}} := \frac{1}{\delta} \mathbf{F}$, (3.10) can be rewritten as

$$\mathcal{G}(\omega, \lambda) \mathbf{y} = \hat{\mathbf{F}}.$$

By continuity of the determinant, $(\mathbf{a}_i(\omega))_{1 \leq i \leq n}$ is a basis of \mathbb{C}^N for ω sufficiently small. This allows us to consider the decomposition of $\mathbf{y} = \mathbf{y}(\omega, \delta)$ onto this basis with coefficients $(y_j(\omega, \delta))_{1 \leq j \leq N}$:

$$\mathbf{y}(\omega, \delta) = \sum_{j=1}^N y_j(\omega, \delta) \mathbf{a}_j(\omega). \quad (4.6)$$

Since $\mathcal{G}(\omega, \lambda_j(\omega)) \mathbf{a}_j(\omega) = 0$, we can write $\mathcal{G}(\omega, \lambda) \mathbf{y}$ as

$$\mathcal{G}(\omega, \lambda) \mathbf{y} = \sum_{i=1}^N y_i(\omega, \delta) (\mathcal{G}(\omega, \lambda) - \mathcal{G}(\omega, \lambda_j(\omega))) \mathbf{a}_i(\omega). \quad (4.7)$$

Then, $\lambda \mapsto (\mathcal{G}(\omega, \lambda) - \mathcal{G}(\omega, \lambda_j(\omega))) \mathbf{a}_j(\omega)$ is analytic in λ and ω and vanishes at $\lambda = \lambda_j(\omega)$. Therefore, this expression can be factorized as

$$(\mathcal{G}(\omega, \lambda) - \mathcal{G}(\omega, \lambda_j(\omega))) \mathbf{a}_j(\omega) = (\lambda - \lambda_j(\omega)) \mathbf{g}_j(\lambda, \omega),$$

for a vector $\mathbf{g}_j(\lambda, \omega)$ analytic in λ and ω . Using the expansion (3.21), we find

$$(\mathcal{G}(\omega, \lambda) - \mathcal{G}(\omega, \lambda_j(\omega))) \mathbf{a}_j(\omega) = -\frac{\lambda - \lambda_j(\omega)}{v_b^2} (\mathbf{a}_j(\omega) + O(\omega^2)),$$

where $O(\omega^2)$ is a function that depends smoothly on λ . Left multiplying (4.7) by $\mathbf{a}_i^T V$ and summing on the indices $1 \leq j \leq N$, we obtain a linear system for the components $(\lambda - \lambda_j(\omega))y_j(\omega, \delta)$:

$$-\sum_{j=1}^N \mathbf{a}_i^T V \mathbf{a}_j(\omega) (1 + O(\omega^2)) \frac{\lambda - \lambda_j(\omega)}{v_b^2} y_j(\omega, \delta) = \mathbf{a}_i^T V \hat{\mathbf{F}}, \quad 1 \leq i \leq N.$$

From (3.27), we have $\mathbf{a}_j^T V \mathbf{a}_i(\omega) = \delta_{ij} + O(\omega)$. This allows to use a Neumann series to invert this linear system, which yields

$$(\lambda - \lambda_j(\omega))y_j(\omega, \delta) = -(1 + O(\omega))v_b^2 \mathbf{a}_i^T V \hat{\mathbf{F}}.$$

Therefore, we find the following expansion for $\mathbf{y}(\omega, \delta)$:

$$\mathbf{y}(\omega, \delta) = -\sum_{j=1}^N \frac{v_b^2}{\lambda - \lambda_j(\omega)} (\mathbf{a}_j^T V \hat{\mathbf{F}}) (1 + O(\omega)) \mathbf{a}_j(\omega).$$

Using $\mathbf{x} = V\mathbf{y}$, and substituting $\lambda = \omega^2/\delta$ and $\hat{\mathbf{F}} = F/\delta$, we obtain

$$\mathbf{x}(\omega, \delta) = -\sum_{j=1}^N \frac{v_b^2}{\omega^2 - \delta\lambda_j(\omega)} (1 + O(\omega)) (\mathbf{a}_j^T V \mathbf{F}) V \mathbf{a}_j.$$

This modal decomposition holds for any complex frequency $\omega \in \mathbb{C}$. If further, ω is real and satisfies $\omega = O(\delta^{\frac{1}{2}})$, then the expansion (3.26) allows to write

$$\begin{aligned} \omega^2 - \delta\lambda_j(\omega) &= \omega^2 - \delta v_b^2 \lambda_j + i\omega \delta \frac{v_b^2}{v} \mathbf{a}_j^T B \mathbf{a}_j + O(\omega^2 \delta) \\ &= \left(\omega^2 - \delta v_b^2 \lambda_j + i\omega \delta \frac{v_b^2}{v} \mathbf{a}_j^T B \mathbf{a}_j \right) \left(1 + O(\delta^{\frac{1}{2}}) \right), \end{aligned}$$

where the order $O(\delta^{\frac{1}{2}})$ can be deduced from [15, Lemma 4.2]. The expansion (4.5) follows. \square

In what follows, we write $(a_{ij})_{1 \leq i, j \leq N} \equiv (\mathbf{a}_1 \quad \mathbf{a}_2 \quad \dots \quad \mathbf{a}_N)$ the coefficients of the column vectors $(\mathbf{a}_j)_{1 \leq j \leq N}$. Inserting the asymptotic (4.5) into (3.13), we obtain the following result.

Proposition 4.3. *Assume that ω is real and belongs to the subwavelength frequency regime $\omega = O(\delta^{\frac{1}{2}})$. The total field $u(\omega, \delta)$ solution to the scattering problem (1.6) admits the following asymptotic modal decomposition in the resonators as $\delta \rightarrow 0$:*

$$u(\omega, \delta) = \frac{\alpha_+ + \alpha_- + O(\delta^{\frac{1}{2}})}{1 - i\tau_M \frac{\omega}{\delta}} + \frac{2i\omega}{v} \sum_{j=2}^N \frac{1}{\lambda_j} \frac{a_{1j}\alpha_+ + a_{Nj}\alpha_- + O(\delta^{\frac{1}{2}})}{\frac{\omega^2}{\omega_{M,j}^2} - 1 + \frac{i\omega}{\lambda_j v} \mathbf{a}_j^T B \mathbf{a}_j} \left(\sum_{i=1}^N a_{ij} 1_{(x_i^-, x_i^+)} \right) \quad \text{in } \prod_{i=1}^N (x_i^-, x_i^+), \quad (4.8)$$

where we have denoted by τ_M the damping constant

$$\tau_M := \frac{v}{2v_b^2} \sum_{p=1}^N \ell_p,$$

and by $\omega_{M,j}$ the first order approximation of the resonant frequency $\omega_j^+(\delta)$:

$$\omega_{M,j} := v_b \lambda_j^{\frac{1}{2}} \delta^{\frac{1}{2}}.$$

Proof. From (3.12) and (4.2), we deduce the following asymptotic for the vector $\mathbf{F} \equiv (F_i)_{1 \leq i \leq N}$:

$$F_i = -\frac{2i\omega\delta}{v} \left(\frac{\alpha_+}{\ell_1} \delta_{i1} + \frac{\alpha_-}{\ell_N} \delta_{iN} \right) + O(\omega^2 \delta),$$

from where we obtain

$$\mathbf{a}_j^T V \mathbf{F} = -\frac{2i\omega\delta}{v} (a_{1j}\alpha_+ + a_{Nj}\alpha_-) + O(\omega^2 \delta).$$

Inserting this expression into (4.5), we obtain the asymptotic expansions of the coordinates of the vector $\mathbf{x}(\omega, \delta) \equiv (x_i(\omega, \delta))_{1 \leq i \leq N}$:

$$\begin{aligned} x_i(\omega, \delta) &= \frac{2i\omega}{v} \sum_{j=1}^N \frac{\delta v_b^2}{\omega^2 - \delta v_b^2 \lambda_j + i\omega \delta \frac{v_b^2}{v} \mathbf{a}_j^T B \mathbf{a}_j} (1 + O(\delta^{\frac{1}{2}})) (a_{1j}\alpha_+ + a_{Nj}\alpha_-) V \mathbf{a}_j \\ &= \frac{2i}{v} \frac{(\alpha_+ + \alpha_- + O(\delta^{\frac{1}{2}}))}{\frac{\omega}{v_b^2 \delta} + 2i \frac{1}{v \sum_{i=p}^N \ell_p}} \frac{1}{\sum_{p=1}^N \ell_p} \ell_i + \frac{2i\omega}{v} \sum_{j=2}^N \frac{1}{\lambda_j} \frac{a_{1j}\alpha_+ + a_{Nj}\alpha_- + O(\delta^{\frac{1}{2}})}{\frac{\omega^2}{\omega_{M,j}^2} - 1 + \frac{i\omega}{\lambda_j v} \mathbf{a}_j^T B \mathbf{a}_j} \ell_i a_{ij} \\ &= \frac{(\alpha_+ + \alpha_- + O(\delta^{\frac{1}{2}}))}{1 - \frac{i\omega v}{2v_b^2 \delta} \sum_{p=1}^N \ell_p} \ell_i + \frac{2i\omega}{v} \sum_{j=2}^N \frac{1}{\lambda_j} \frac{a_{1j}\alpha_+ + a_{Nj}\alpha_- + O(\delta^{\frac{1}{2}})}{\frac{\omega^2}{\omega_{M,j}^2} - 1 + \frac{i\omega}{\lambda_j v} \mathbf{a}_j^T B \mathbf{a}_j} \ell_i a_{ij}. \end{aligned}$$

Using the expansion (3.15) for the modal functions $u_j(\omega, \delta)$, equation (3.13) allows to infer the following approximation for $u(\omega, \delta)$ on $\bigsqcup_{i=1}^N (x_i^-, x_i^+)$:

$$\begin{aligned} u(\omega, \delta) &= O(\omega\delta) + \sum_{i=1}^N \left(\frac{(\alpha_+ + \alpha_- + O(\delta^{\frac{1}{2}}))}{1 - \frac{i\omega v}{2v_b^2\delta} \sum_{p=1}^N \ell_p} + \frac{2i\omega}{v} \sum_{j=2}^N \frac{1}{\lambda_j} \frac{a_{1j}\alpha_+ + a_{Nj}\alpha_- + O(\delta^{\frac{1}{2}})}{\frac{\omega^2}{\omega_{M,j}^2} - 1 + \frac{i\omega}{\lambda_j v} \mathbf{a}_j^T \mathbf{B} \mathbf{a}_j} a_{ij} \right) \mathbf{1}_{(x_i^-, x_i^+)} \\ &= \frac{\alpha_+ + \alpha_- + O(\delta^{\frac{1}{2}})}{1 - i\tau_M \frac{\omega}{\delta}} + \frac{2i\omega}{v} \sum_{j=2}^N \frac{1}{\lambda_j} \frac{a_{1j}\alpha_+ + a_{Nj}\alpha_- + O(\delta^{\frac{1}{2}})}{\frac{\omega^2}{\omega_{M,j}^2} - 1 + \frac{i\omega}{\lambda_j v} \mathbf{a}_j^T \mathbf{B} \mathbf{a}_j} \sum_{i=1}^N a_{ij} \mathbf{1}_{(x_i^-, x_i^+)}. \end{aligned}$$

□

The result of Proposition 4.3 shows that the constant mode is excited in the regime $\omega = O(\delta)$, while piecewise constant modes are excited around the frequency $\omega \simeq \omega_{M,j}$. For $2 \leq j \leq N$, the j -th mode is constant in each resonator (x_i^-, x_i^+) , with a constant given by the i -th coefficient of the eigenvector \mathbf{a}_j of the capacitance eigenvalue problem (3.22).

4.2. Transmission and reflection coefficients of the high-contrast medium

The next proposition motivates the definition of the transmission and reflection coefficients.

Proposition 4.4. *Let us assume that ω is real and that u_{in} is a wave propagating from left to right, namely $\alpha_- = 0$ in (4.1). Then we have the following energy conservation identity:*

$$\left| \frac{u(x_1^-) - u_{\text{in}}(x_1^-)}{u_{\text{in}}(x_1^-)} \right|^2 + \left| \frac{u(x_N^+)}{u_{\text{in}}(x_N^+)} \right|^2 = 1. \quad (4.9)$$

Proof. The total field u solution to (1.6) satisfies

$$-\frac{d}{dx} \left[\frac{1}{\rho(x)} \frac{d}{dx} u \right] - \frac{\omega^2}{\kappa(x)} u = 0 \text{ in } \mathbb{R},$$

where we recall the definition (1.2) of $\kappa(x)$ and $\rho(x)$. Multiplying by the conjugate \bar{u} and integrating by parts on (x_1^-, x_N^+) yields

$$\int_{x_1^-}^{x_N^+} \left[\frac{1}{\rho(x)} \left| \frac{d}{dx} u(x) \right|^2 - \frac{\omega^2}{\kappa(x)} |u(x)|^2 \right] dx - \frac{1}{\rho_b} \frac{du}{dx}(x_N^+) \bar{u}(x_N^+) + \frac{1}{\rho_b} \frac{du}{dx}(x_1^-) \bar{u}(x_1^-) = 0, \quad (4.10)$$

where we used the jump relations of (1.6) to cancel the terms occuring at intermediate points. Since u_{in} propagates from left to right, we have $du_{\text{in}}/dx = ik u_{\text{in}}$. We now remark that

$$\frac{du}{dx}(x_N^+) = \frac{d(u - u_{\text{in}})}{dx}(x_N^+) + \frac{du_{\text{in}}}{dx}(x_N^+) = ik(u(x_N^+) - u_{\text{in}}(x_N^+)) + ik u_{\text{in}}(x_N^+) = ik u(x_N^+),$$

and

$$\frac{du}{dx}(x_1^-) = \frac{d(u - u_{\text{in}})}{dx}(x_1^-) + \frac{du_{\text{in}}}{dx}(x_1^-) = -ik(u(x_1^-) - u_{\text{in}}(x_1^-)) + ik u_{\text{in}}(x_1^-).$$

Inserting these values into (4.10) and taking the imaginary part yields

$$\begin{aligned} 0 &= -|u(x_N^+)|^2 + [-(u(x_1^-) - u_{\text{in}}(x_1^-)) + u_{\text{in}}(x_1^-)]((\bar{u}(x_1^-) - \bar{u}_{\text{in}}(x_1^-)) + \bar{u}_{\text{in}}(x_1^-)) \\ &= -|u(x_N^+)|^2 - |u(x_1^-) - u_{\text{in}}(x_1^-)|^2 + |u_{\text{in}}(x_1^-)|^2, \end{aligned}$$

which concludes the proof. □

Motivated by the energy identity (4.9), we introduce the transmission and reflection coefficients as follows.

Definition 4.1. Consider an incident wave u_{in} propagating from left to right. The transmission and the reflection coefficients of the system of N resonators are the complex quantities $T(\omega, \delta)$ and $R(\omega, \delta)$ defined by

$$T(\omega, \delta) := \frac{u(x_N^+)}{u_{\text{in}}(x_N^+)}, \quad R(\omega, \delta) := \frac{u(x_1^-) - u_{\text{in}}(x_1^-)}{u_{\text{in}}(x_1^-)}. \quad (4.11)$$

The coefficients $T(\omega, \delta)$ and $R(\omega, \delta)$ capture the amplitude and the phase (or time delay with respect to the incident wave) of the transmitted reflected waves, which are respectively the parts of the solution u which propagate from left to right and from right to left. The identity (4.9) reads

$$|T(\omega, \delta)|^2 + |R(\omega, \delta)|^2 = 1,$$

which implies in particular that $T(\omega, \delta)$ and $R(\omega, \delta)$ are of modulus lower than one.

In the next proposition, we compute the leading asymptotic expansions of $T(\omega, \delta)$ and $R(\omega, \delta)$.

Proposition 4.5. Assume that ω is real and $\omega = O(\delta^{\frac{1}{2}})$. The reflection and transmission coefficients $T(\omega, \delta)$ and $R(\omega, \delta)$ of (4.11) have the following asymptotic expansions:

$$T(\omega, \delta) = \frac{1 + O(\delta^{\frac{1}{2}})}{1 - i\tau_M \frac{\omega}{\delta}} + \frac{2i\omega}{v} \sum_{j=2}^N \frac{1}{\lambda_j} \frac{a_{1j} a_{Nj} + O(\delta^{\frac{1}{2}})}{\frac{\omega^2}{\omega_{M,j}^2} - 1 + \frac{i\omega}{\lambda_j v} \mathbf{a}_j^T \mathbf{B} \mathbf{a}_j},$$

$$R(\omega, \delta) = \frac{1 + O(\delta^{\frac{1}{2}})}{1 - i\tau_M \frac{\omega}{\delta}} + \frac{2i\omega}{v} \sum_{j=2}^N \frac{1}{\lambda_j} \frac{a_{1j}^2 + O(\delta^{\frac{1}{2}})}{\frac{\omega^2}{\omega_{M,j}^2} - 1 + \frac{i\omega}{\lambda_j v} \mathbf{a}_j^T \mathbf{B} \mathbf{a}_j} - 1.$$

Proof. From (4.8) with $u_{\text{in}}(x) = \alpha_+ e^{ikx}$, we infer that

$$u(x_N^+) = \frac{\alpha_+}{1 - i\tau_M \frac{\omega}{\delta}} + \frac{2i\omega}{v} \sum_{j=2}^N \frac{1}{\lambda_j} \frac{a_{1j} \alpha_+ + O(\delta^{\frac{1}{2}})}{\frac{\omega^2}{\omega_{M,j}^2} - 1 + \frac{i\omega}{\lambda_j v} \mathbf{a}_j^T \mathbf{B} \mathbf{a}_j} a_{Nj} + O(\delta^{\frac{1}{2}}).$$

Hence, the transmission coefficient reads

$$T(\omega, \delta) = \frac{u(x_N^+)}{u_{\text{in}}(x_N^+)} = \left(\frac{1}{1 - i\tau_M \frac{\omega}{\delta}} + \frac{2i\omega}{v} \sum_{j=2}^N \frac{1}{\lambda_j} \frac{a_{1j} a_{Nj} + O(\delta^{\frac{1}{2}})}{\frac{\omega^2}{\omega_{M,j}^2} - 1 + \frac{i\omega}{\lambda_j v} \mathbf{a}_j^T \mathbf{B} \mathbf{a}_j} + O(\delta^{\frac{1}{2}}) \right) e^{-ikx_N^+},$$

and the expression for $T(\omega, \delta)$ follows, observing that $e^{-ikx_N^+} = 1 + O(\delta^{\frac{1}{2}})$. Similarly,

$$u(x_1^-) = \frac{\alpha_+}{1 - i\tau_M \frac{\omega}{\delta}} + \frac{2i\omega}{v} \sum_{j=2}^N \frac{1}{\lambda_j} \frac{a_{1j} \alpha_+ + O(\delta^{\frac{1}{2}})}{\frac{\omega^2}{\omega_{M,j}^2} - 1 + \frac{i\omega}{\lambda_j v} \mathbf{a}_j^T \mathbf{B} \mathbf{a}_j} a_{1j} + O(\delta^{\frac{1}{2}}),$$

which yields the reflection coefficient

$$R(\omega, \delta) = \frac{u(x_1^-) - u_{\text{in}}(x_1^-)}{u_{\text{in}}(x_1^-)} = \frac{1 + O(\delta^{\frac{1}{2}})}{1 - i\tau_M \frac{\omega}{\delta}} + \frac{2i\omega}{v} \sum_{j=2}^N \frac{1}{\lambda_j} \frac{a_{1j}^2 + O(\delta^{\frac{1}{2}})}{\frac{\omega^2}{\omega_{M,j}^2} - 1 + \frac{i\omega}{\lambda_j v} \mathbf{a}_j^T \mathbf{B} \mathbf{a}_j} - 1.$$

□

Remark 4.2. In the single resonator case $N = 1$, the transmission and the reflection coefficients can be explicitly written as

$$R(\omega, \delta) = \frac{(\delta^2 v_b^2 - v^2) \sin\left(\frac{\omega \ell_1}{v_b}\right)}{(\delta^2 v_b^2 + v^2) \sin\left(\frac{\omega \ell_1}{v_b}\right) + 2i\delta v v_b \cos\left(\frac{\omega \ell_1}{v_b}\right)},$$

$$T(\omega, \delta) = \frac{2i\delta v v_b}{(\delta^2 v_b^2 + v^2) \sin\left(\frac{\omega \ell_1}{v_b}\right) + 2i\delta v v_b \cos\left(\frac{\omega \ell_1}{v_b}\right)}.$$
(4.12)

Considering incident frequencies $\omega \sim v_b \lambda_j^{\frac{1}{2}} \delta^{\frac{1}{2}}$ close to the resonant values, we obtain the following result for the transmission and reflection coefficients near the resonant frequencies.

Corollary 4.1. The transmission and reflection coefficients converge to the following values near the resonant frequencies:

- the following convergences hold as $\omega = o(\delta)$ with $\delta \rightarrow 0$:

$$T(0, \delta) \rightarrow 1, \quad R(0, \delta) \rightarrow 0;$$

- the following convergences hold as $\delta \rightarrow 0$ with $\omega \sim v_b \lambda_j^{\frac{1}{2}} \delta^{\frac{1}{2}}$:

$$T(\omega, \delta) \rightarrow T_j \text{ and } R(\omega, \delta) \rightarrow R_j,$$

where the limit transmission and reflection coefficients T_j and R_j are given by

$$T_j := \frac{2a_{1j} a_{Nj}}{a_{1j}^2 + a_{Nj}^2}, \quad R_j := \frac{a_{1j}^2 - a_{Nj}^2}{a_{1j}^2 + a_{Nj}^2}.$$
(4.13)

Here, we recall the notation $(a_{ij})_{1 \leq i \leq N}$ for the coefficients of the eigenvector \mathbf{a}_j of (3.22).

- If $\omega = O(\delta^{\frac{1}{2}})$ stays away from the resonant frequencies, namely if

$$\omega \gg \delta \text{ and } |\omega - v_b \lambda_j^{\frac{1}{2}} \delta^{\frac{1}{2}}| \gg \delta \text{ for any } 2 \leq j \leq N,$$

then

$$T(\omega, \delta) \rightarrow 0 \text{ and } R(\omega, \delta) \rightarrow -1.$$

Remark 4.3. The corollary shows that the transmission is optimal near the resonant frequency $\omega_j(\delta)$ when the first and last entries of the eigenvector \mathbf{a}_j coincide, up to a sign. Furthermore, the last point of the corollary states that away from a band around the resonances of size $O(\delta)$, the reflection coefficient remains close to -1 . The formula (4.13) suggests that exceptional positive reflection coefficients can be obtained near the resonances $\omega_{M,j}$ upon the condition $a_{Nj} = 0$. We present in the next section several numerical evidences of these results.

5. NUMERICAL ILLUSTRATIONS OF SUBWAVELENGTH RESONANCES

In this final section, we provide several numerical illustrations of the subwavelength resonant phenomena occurring in the 1D high-contrast system of Figure 1. We consider four different situations with a system of $N = 1, 2, 6$ non-identical resonators, and a system of 6 identical resonators, which are respectively treated in Sections 5.2 to 5.5. The values of the physical parameters considered, as well as the adopted numerical methodology are first detailed in Section 5.1.

5.1. Setting and methodology

In all three situations, the physical parameters are set to

$$v = 1, \quad v_b = 1, \quad \delta = 0.001,$$

while the frequency ω is a parameter that is allowed to vary in a “subwavelength” frequency range $(0, \Omega)$. In the present 1D setting, a natural choice for the bound Ω is

$$\Omega := 0.1 \frac{\pi}{\max_{1 \leq i \leq N} \ell_i}. \quad (5.1)$$

Indeed, frequencies larger than Ω correspond to wavelengths smaller or comparable to the size of the largest resonator, hence they cannot be qualified “subwavelength”. More mathematically said, the first nonzero Neumann eigenvalue of the (negative) Laplacian operator on $\bigsqcup_{i=1}^N (x_i^-, x_i^+)$ is $\pi / \max_{1 \leq i \leq N} \ell_i$, around which further resonances (called Fabry-Pérot resonances, see [13]) occur.

In all three situations, we consider an incident wave propagating from left to right:

$$u_{\text{in}}(x) = e^{ikx}, \quad (5.2)$$

where we recall that $k = \omega/v$. We solve numerically the scattering problem (1.6) with u_{in} given by (5.2), and we compute the transmission and reflection coefficients for incident frequencies in the subwavelength regime $(0, \Omega)$. We observe peaks of the transmission coefficient at the subwavelength resonant frequencies predicted by the asymptotic analysis of Proposition 3.3. Furthermore, we also verify the result of Corollary 4.1 which states that for $\omega \simeq \omega_{M,j} = v_b \lambda_j^{\frac{1}{2}} \delta^{\frac{1}{2}}$, the transmission and reflection coefficients converge to the quantities T_j and R_j of (4.13).

Our discussions include plots of the numerical solution u to the scattering problem (1.6), which are obtained by plotting the function $x \mapsto \Re(u(x)e^{-i\phi})$, where ϕ is a phase shift selected to observe the maximum amplitude of the wave on the negative real line:

$$e^{i\phi} := \frac{u(0)}{|u(0)|}. \quad (5.3)$$

This phase shift allows the reader to better appreciate the damping or the enhancement of the transmitted wave near the resonances.

In order to assess the accuracy of the asymptotic formula of Proposition 3.3, we compute numerically the exact values of the subwavelength resonant frequencies with the Muller’s method [30], following the methodology of [9, Section 1.6], and report their values in Tables 1 to 4 below. We rely on the implementation provided by the open-source code [34]. We recall that the Muller’s method allows to find (complex) roots of holomorphic functions by using quadratic interpolants. In our case, we apply the Muller’s method to obtain the zeros of the function $\omega \mapsto \mu_1(\omega)$, where $\mu_1(\omega)$ is the eigenvalue of the matrix $\mathcal{A}(\omega, \delta)$ (Eq. (3.3)) with the smallest complex modulus. Since $\mu_1(\omega) = 0$ implies that $\mathcal{A}(\omega, \delta)$ is not invertible, computing such roots ω yields the desired resonant frequencies. In order to obtain all the roots, we initialize the Muller’s method with the frequencies (3.23) and (3.24) predicted by the asymptotic analysis.

The numerical results allow to observe the arising of subwavelength resonances, which are frequencies for which the transmission coefficient becomes suddenly close to a nonzero value. In contrast, there is almost no transmission to the positive real line when the incident frequency is away from the resonances, leading to almost perfect reflection. It is also possible to observe special resonances (see e.g. $\omega_5^+(\delta)$ in Section 5.4) with low transmission but a positive reflection coefficient ($R(\omega, \delta) \simeq +1$ instead of $R(\omega, \delta) \simeq -1$ away from the resonances). These findings show that such systems of subwavelength resonators can serve as a low pass filter for frequencies very close to zero, and as either a band filter near the nonzero resonant frequencies, or an amplifier of the reflected wave.

Frequency	Theoretical	Numerical	T_j	R_j
$\omega_0(\delta)$	0	0	1	0
$\omega_1(\delta)$	$-0.0020000006666670215i$	$-0.0020000006666698773i$	1	0

TABLE 1. Theoretical frequencies predicted by the leading-order approximation of [Proposition 3.3](#) for the single resonator setting of [Section 5.2](#). The last column features the predicted transmission and reflection coefficients $(T_j)_{1 \leq j \leq N}$ and $(R_j)_{1 \leq j \leq N}$ around resonant frequencies according to [\(4.13\)](#).

5.2. Single resonator case

Our first example is the simplest situation in which there is only a single resonator of unit length $\ell_1 = 1$, as illustrated on [Figure 3](#). The system admits only the null frequency $\omega_0(\delta) = 0$ and a purely imaginary resonant

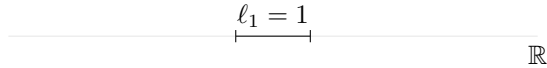


FIGURE 3. A situation with a single $N = 1$ subwavelength resonator.

frequency $\omega_1(\delta) \in i\mathbb{R}$. We compare in [Table 1](#) the numerical value obtained with the Muller's method for the purely imaginary frequency ω_1 to the predicted exact value given in [\(3.28\)](#), which are in excellent agreement.

We then plot on [Figure 4](#) the real part of the transmission and the reflection coefficients defined in [\(4.11\)](#). In the present situation with $N = 1$, the formula [\(5.1\)](#) yields $\Omega \simeq 0.31$. We observe the absence of distinguished subwavelength resonances apart from the peak at $\omega = 0$. In order to illustrate this behaviour, we compute the total wave solution at the frequencies $\omega \in \{0.003, 0.05\}$ and plot on [Figure 5](#) the respective solution function $x \mapsto \Re(u(x)e^{-i\phi})$, where ϕ is the phase shift [\(5.3\)](#). We clearly observe that the transmitted wave is considerably damped at $\omega = 0.05$, while a significant part of the wave is transmitted on the positive real line in the first case $\omega = 0.003$.

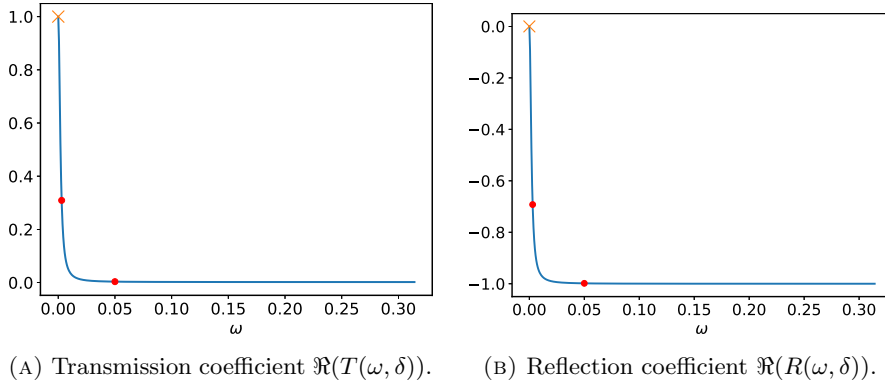


FIGURE 4. Transmission and reflection coefficients (Eq. [\(4.11\)](#)) for the single resonator case of [Section 5.2](#). The red dots indicate the frequencies $\omega = 0.003$ and $\omega = 0.05$, whose associated solution waves are plotted on [Figure 5](#).

Finally, we plot on [Figure 6](#) the resonant modes associated with $\omega_0(\delta) = 0$ and $\omega_1(\delta)$, obtained with the Muller's method. The mode associated to $\omega_0(\delta)$ is uniformly constant on \mathbb{R} , while the mode associated to $\omega_1(\delta) \in i\mathbb{R}$ has an exponential spatial growth.

To summarize, these numerical computations illustrate the fact that a single subwavelength resonator behaves as a low pass filter in the subwavelength frequency regime.

5.3. Two resonator case

Our second example is a situation featuring two resonators with different sizes: the precise setting is given on [Figure 7](#). The transmission and reflection coefficients associated to the incident wave [\(5.2\)](#) are plotted on [Figure 8](#) on the frequency range $\omega \in (0, \Omega)$, for which the formula [\(5.1\)](#) yields $\Omega \simeq 0.079$. The plots reveal the occurrence of a non-trivial, nonzero resonant frequency $\omega_2^+(\delta)$ in this subwavelength range. We then check that the peak observed in the transmission coefficient occurs near the resonances predicted by the asymptotic analysis of [Propositions 3.3](#) and [4.5](#): we report in [Table 2](#) the numerical values of the subwavelength resonant

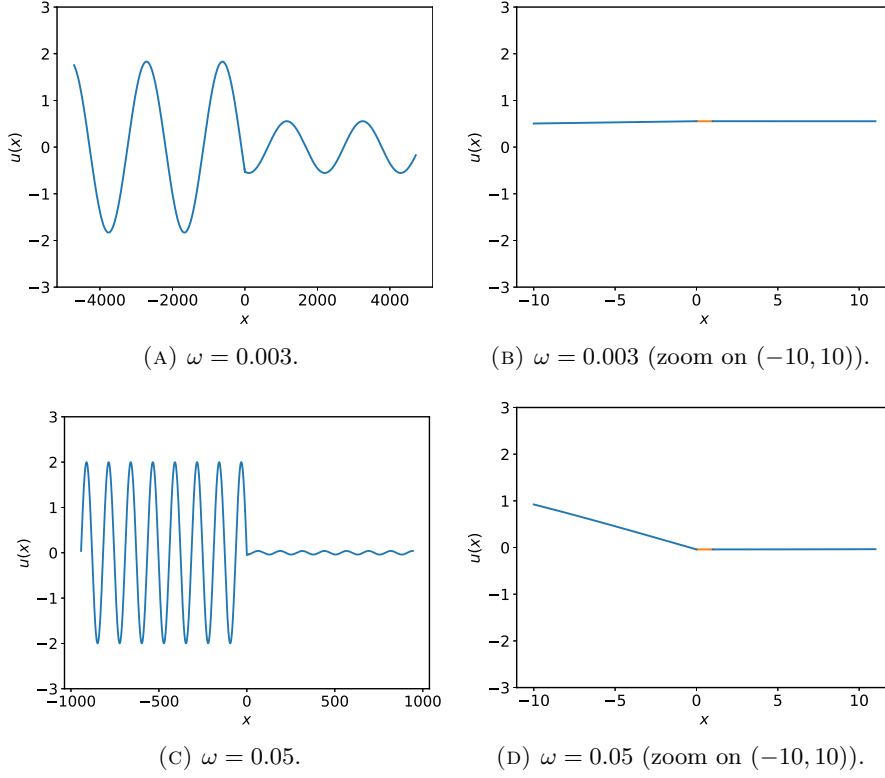


FIGURE 5. Wave $\Re(u(x)e^{-i\phi})$ solution to (1.7) for two incident frequencies $\omega = 0.003$ and $\omega = 0.05$ (reported as the red dots on Figure 4), in the single resonator case of Section 5.2. For both frequencies, we plot a zoom of the solution on the interval $(-10, 10)$. The part of the solution on the resonator (x_1^-, x_1^+) is represented in orange color. The phase ϕ is chosen according to (5.3).

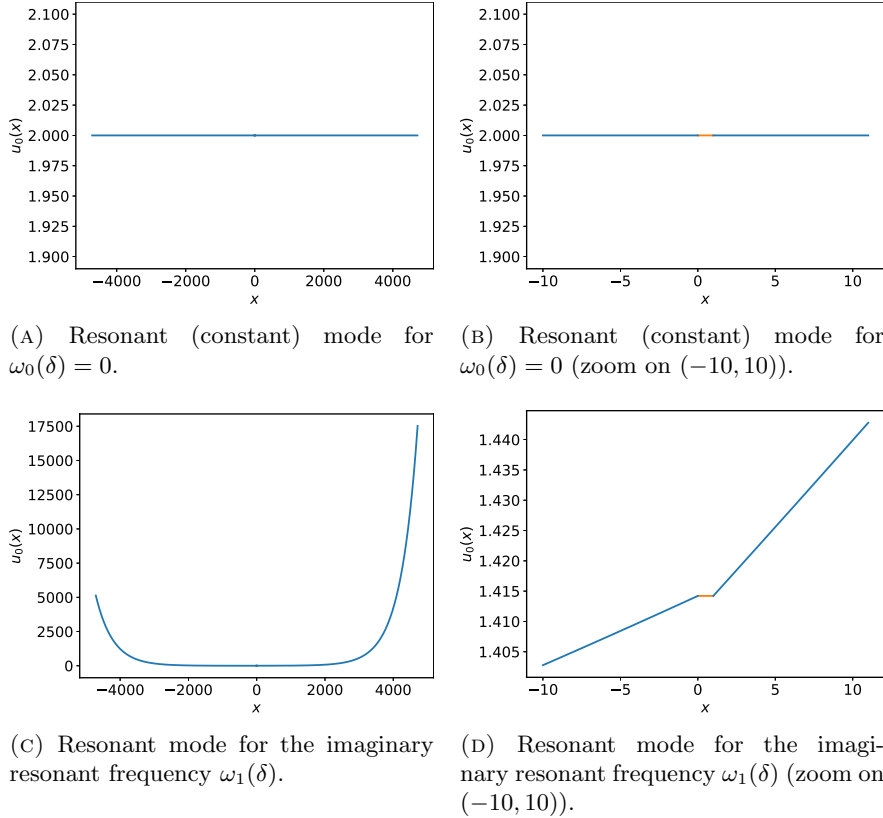
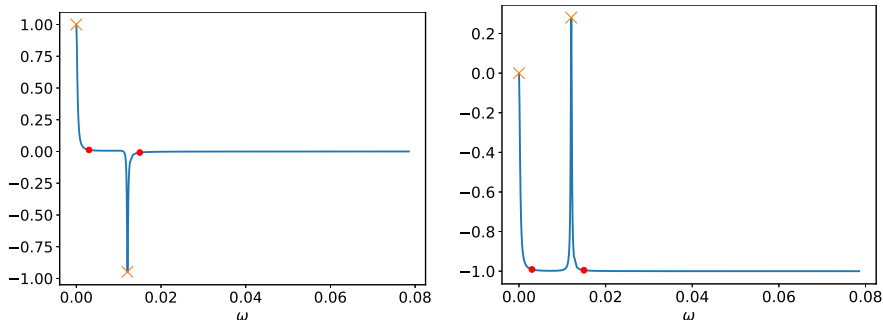


FIGURE 6. Subwavelength resonant modes for the single resonator case of Section 5.2.

FIGURE 7. A situation with $N = 2$ subwavelength resonators.(A) Transmission coefficient $\Re(T(\omega, \delta))$. (B) Reflection coefficient $\Re(R(\omega, \delta))$.FIGURE 8. Transmission and reflection coefficients (Eq. (4.11)) for the two resonator case of Section 5.3. The red dots indicate the frequencies $\omega = 0.02$ and $\omega = 0.15$, while the orange cross marks the predicted resonant frequency $\omega_2^+(\delta) \simeq 0.0382$. The wave solutions associated to these frequencies are plotted on Figure 9.

Frequency	Theoretical	Numerical	T_j	R_j
$\omega_0(\delta)$	0	0	1	0
$\omega_1(\delta)$	$-0.00028571i$	$-0.00028555i$	1	0
$\omega_2^+(\delta)$	$0.012076 - 0.00014881i$	$0.012070 - 0.00014886i$	-0.96	0.28

TABLE 2. Theoretical frequencies predicted by the leading-order approximation of Proposition 3.3 for the two resonator case of Section 5.3. The last column feature the predicted transmission and reflection coefficients $(T_j)_{1 \leq j \leq N}$ and $(R_j)_{1 \leq j \leq N}$ around resonant frequencies according to (4.13).

frequencies computed with the Muller's method, and compare them to the formulas (3.23) and (3.24). The real part of the predicted value for the resonant frequency $\omega_2^+(\delta)$ is also indicated by an orange cross on the transmission and reflection plots of Figure 8. Despite the fact that we use only the leading-order asymptotic in δ , we still observe a very good agreement between the numerical and theoretical values. To illustrate the behavior of the system around the resonant frequency $\omega_2^+(\delta)$, we plot on Figure 9 the total wave field for the three different frequencies $\omega \in \{0.003, 0.0121, 0.015\}$, which are marked on Figure 8 with the red points and orange crosses. We still use the phase shift (5.3) to display the maximum values attained by the incident wave. We clearly observe the significant enhancement of transmission near the resonant frequency $\omega_1^+(\delta) \simeq 0.0121$, and the damping of the transmitted wave (on the positive real line) at the frequencies $\omega \in \{0.003, 0.015\}$. The imperfect transmission value $T_2 \simeq -0.96$ comes from the lack of symmetry of the system. We can appraise the fact that the resonators (x_1^-, x_1^+) and (x_2^-, x_2^+) operate in the subwavelength frequency regime: for instance they are approximately a hundred times smaller than the operating wavelength on Figure 9c!

Finally, we plot on Figure 10 the resonant modes associated to the three resonant frequencies $\omega_0(\delta) = 0$, $\omega_1(\delta) \in i\mathbb{R}$ and $\omega_2(\delta)^+$. The mode associated to $\omega_1(\delta)$ exhibits no oscillation but a slow exponential growth. The mode associated to $\omega_2^+(\delta)$ has an oscillating component and a slow exponential growth. We remark that, consistently with the approximation formula (4.8), the total solution at $\omega = 0.0121 \simeq \omega_2^+(\delta)$ visible on Figure 9c resembles to the resonant mode visible on Figure 10e.

To conclude, these numerical results illustrate the fact that in this situation, the system behaves as a low pass filter very close to the null frequency $\omega_0(\delta) = 0$, and as a band pass filter close to the resonant frequency $\omega_2^+(\delta)$.

5.4. Six resonator case

In order to illustrate the fact that the 1D system of Figure 3 admits exactly as many subwavelength resonances as the number N of subwavelength resonators (one of them being located at the null frequency $\omega_0(\delta) = 0$), we consider now a situation with six resonators, illustrated on Figure 11. The transmission and reflection coefficients associated to the incident wave (5.2) are plotted on Figure 12. As expected from the result of

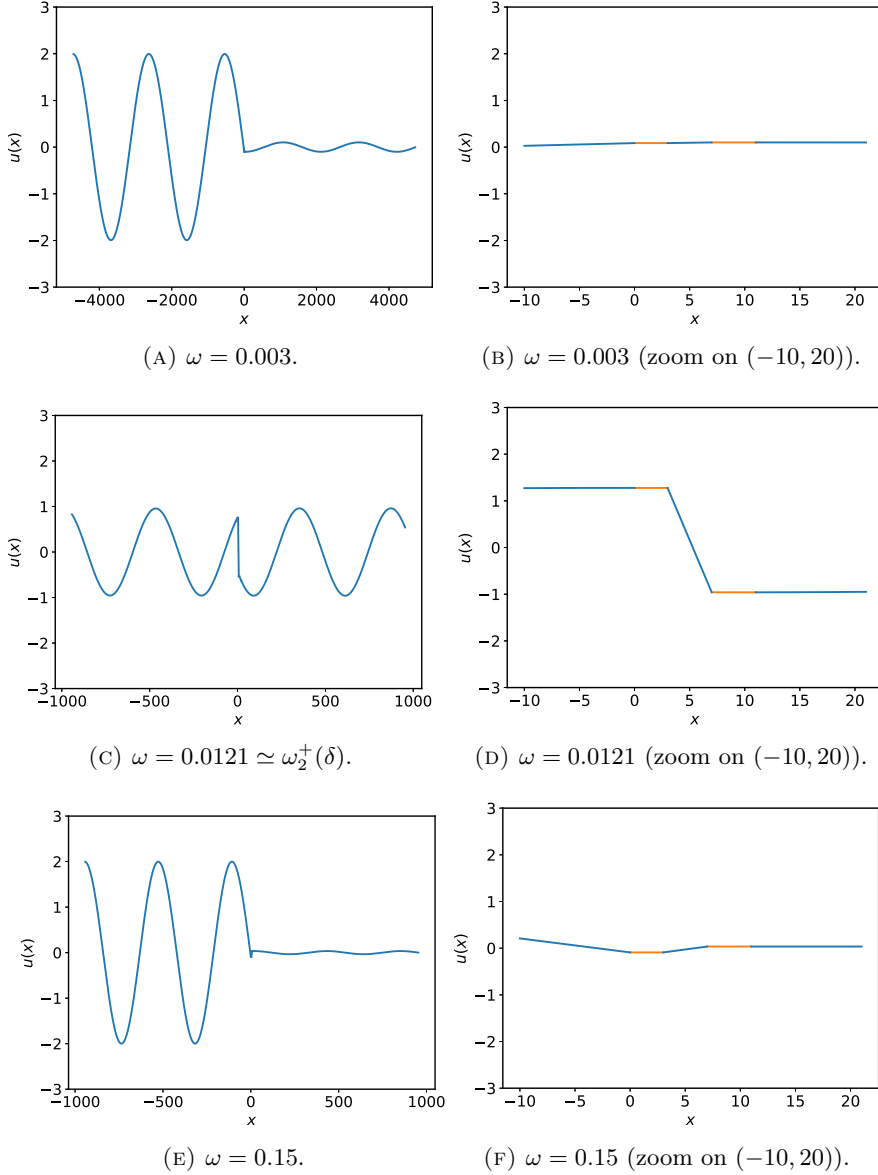


FIGURE 9. Wave solution $\Re(u(x)e^{-i\phi})$ to (1.7) for three incident frequencies $\omega \in \{0.003, 0.0121, 0.15\}$ in the two resonator setting of Section 5.3. These frequencies, reported with the red mark and the orange crosses on Figure 8, are either far from or close to the resonances. The part of the solution crossing the resonators is drawn in orange color. The phase ϕ is chosen according to (5.3).

Proposition 3.3, six resonant frequencies are visible, including the zero frequency $\omega_0(\delta) = 0$. The magnitude of the resonant peaks decay as the order of the resonance increases, which is consistent with the transmission coefficients values T_j reported in Table 3. A striking feature of this system is the fifth resonance $\omega_5^+(\delta)$ which is associated to a reflection coefficient $R_5 \simeq 0.93$ close to the value $+1$, instead of the value -1 encountered away from the resonances.

We report on Table 3 the numerical values of the subwavelength resonant frequencies computed with the Muller's method, and compare them to the values obtained with formulas (3.23) and (3.24). We also report the predicted frequencies with an orange cross on the transmission and reflections plots of Figure 8. Once again, we observe that the numerical and theoretical values are in very good agreement, up to a slight loss of accuracy for the imaginary part of the highest order resonant frequencies $\omega_5^+(\delta)$ and $\omega_6^+(\delta)$. We then plot on Figure 13 the total wave field generated by the incident wave (5.2) at the frequencies $\omega \in \{0.0119, 0.0165, 0.0197, 0.0272\}$ which are respectively close to $\omega_3^+(\delta)$, in between $\omega_3^+(\delta)$ and $\omega_4^+(\delta)$, close to $\omega_4^+(\delta)$ and close to $\omega_5^+(\delta)$. Their values are indicated by the red mark and the orange crosses on Figure 12. Again, we observe that the incident wave is transmitted to the right part of the domain for frequencies close to the first four resonant frequencies: the magnitude of the transmitted wave field on the positive real line is large for $\omega \simeq \omega_3^+(\delta)$ and $\omega \simeq \omega_4^+(\delta)$, and slightly damped for $\omega = 0.0272 \simeq \omega_5^+(\delta)$. The attenuation observed for $\omega = 0.0272$ is consistent with the value $T_5 \simeq 0.37$ of the transmission coefficient. However, we observe the striking amplified and inverted reflected wave

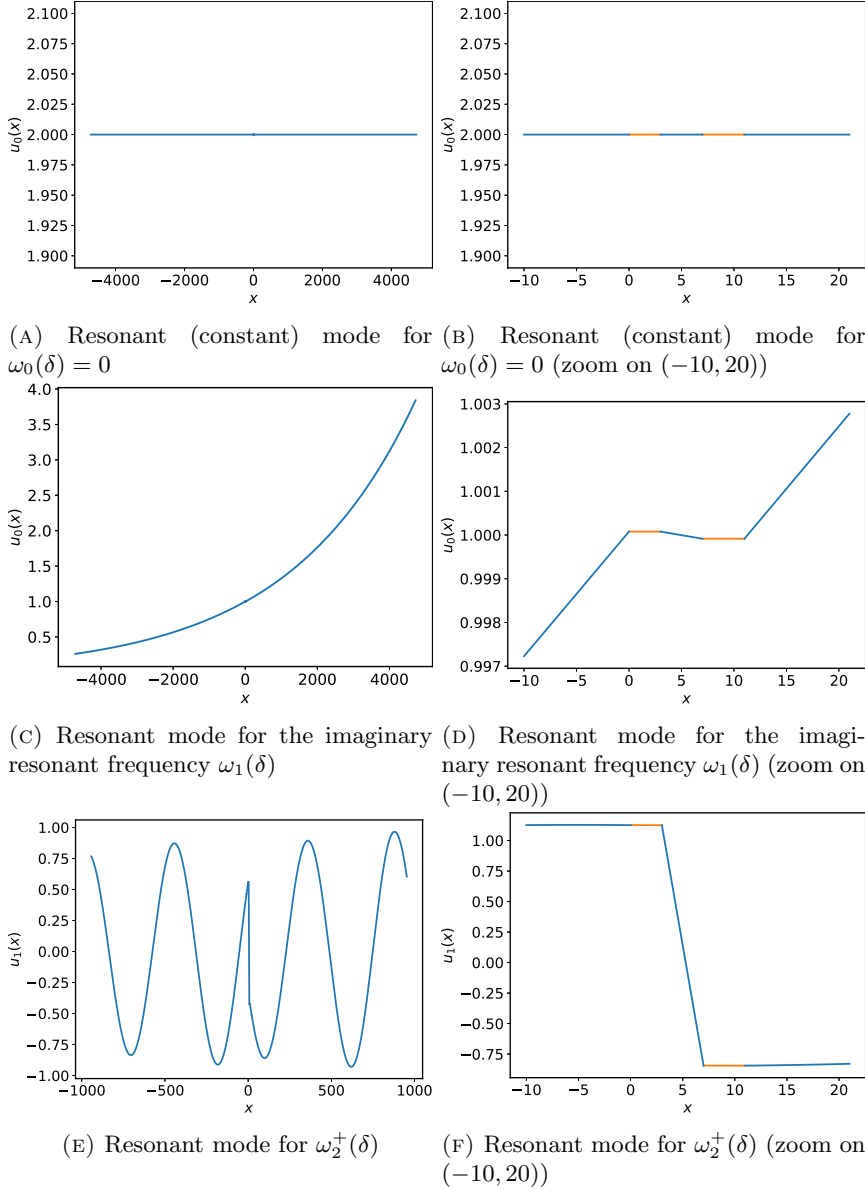


FIGURE 10. Subwavelength resonant modes for the two resonator case of Section 5.3.

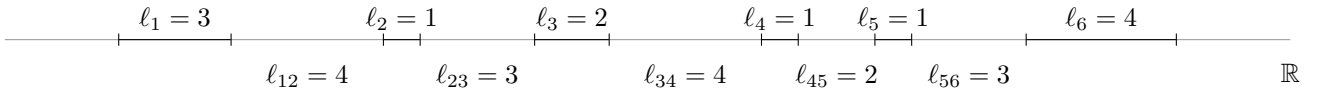


FIGURE 11. A situation with $N = 6$ subwavelength resonators.

on Figure 13g. Finally, we report on Figure 14 the six resonant modes computed with the Muller's method associated to the six subwavelength resonant frequencies. The first mode is constant, the second has a slow exponential growth and no oscillatory behavior, while the subsequent ones feature both a slow exponential growth and an oscillatory behavior. Consistently with the analysis of Proposition 3.3, the total wave fields are approximately constants in the resonators, with constants being approximately proportional to the coordinates of the eigenvectors $(\mathbf{a}_i)_{1 \leq i \leq N}$ of the capacitance eigenvalue problem (3.22). We still remark the resemblance of the wave solution u at $\omega \simeq \omega_3^+(\delta)$ and $\omega \simeq \omega_4^+(\delta)$ (Figs. 17a and 17e) to the modes associated to these frequencies (Figs. 14g and 14i), up to a phase shift.

To conclude, this numerical experiment further illustrates the arising of as many resonances as the number of considered resonators, the ability of the resonators to manipulate waves at subwavelength scales, and the fact that the transmission and reflection properties are well predicted by the capacitance analysis of Proposition 3.3.

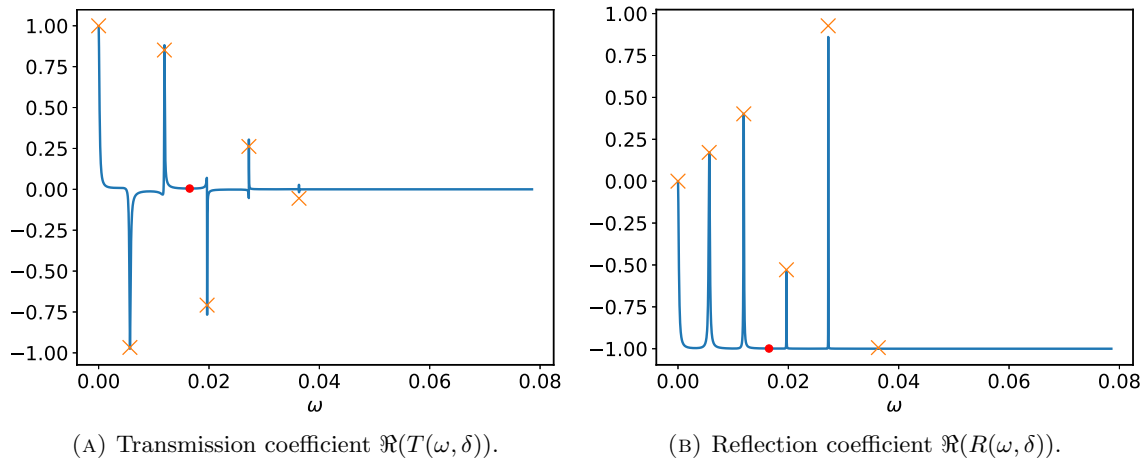


FIGURE 12. Transmission and reflection coefficients (Eq. (4.11)) for the six resonator case of Section 5.4. The red dot indicates the frequency $\omega = 0.0165$, while the orange cross indicates the location of the predicted resonant frequencies (from Table 3). The wave solutions associated to the frequencies marked by the red dots and $\omega_3^+(\delta)$ and $\omega_4^+(\delta)$ are plotted on Figure 13.

Frequency	Theoretical	Numerical	T_j	R_j
$\omega_0(\delta)$	0	0	1	0
$\omega_1(\delta)$	$-0.00016667i$	$-0.00016647i$	1	0
$\omega_2^+(\delta)$	$0.005669 - 0.00012768i$	$0.0056643 - 0.00012759i$	-0.985	0.172
$\omega_3^+(\delta)$	$0.011926 - 5.8224 \times 10^{-5}i$	$0.011915 - 5.8286 \times 10^{-5}i$	0.915	0.403
$\omega_4^+(\delta)$	$0.019678 - 1.5263 \times 10^{-5}i$	$0.019658 - 1.5326 \times 10^{-5}i$	-0.848	-0.530
$\omega_5^+(\delta)$	$0.027254 - 5.9817 \times 10^{-6}i$	$0.027229 - 6.0172 \times 10^{-6}i$	0.371	0.929
$\omega_6^+(\delta)$	$0.036341 - 1.1878 \times 10^{-6}i$	$0.036311 - 1.2017 \times 10^{-6}i$	-0.113	-0.994

TABLE 3. Theoretical frequencies predicted by the leading-order approximation of Proposition 3.3 for the six resonator case of Section 5.4. The last column features the predicted transmission and reflection coefficients $(T_j)_{1 \leq j \leq N}$ and $(R_j)_{1 \leq j \leq N}$ around resonant frequencies according to (4.13).

5.5. Six resonator case with perfect transmission

We now consider a final example to illustrate the possibility to achieve perfect transmission and zero reflection near the resonant frequencies. As highlighted from the formula (4.13), the loss of transmission near resonances is due to the difference between the first and the last entries of the eigenvectors \mathbf{a}_j of the capacitance eigenvalue problem (3.22). If the system of resonators is invariant when reversing the direction of the real line (i.e. under the inversion of the order of the sequences $(\ell_i)_{1 \leq i \leq N}$ and $(\ell_{i(i+1)})_{1 \leq i \leq N-1}$), then it can be shown by using a symmetry argument that the same symmetry property holds for the eigenvectors \mathbf{a}_j , up to a change of sign.

Proposition 5.1. *Assume that the sequences $(\ell_i)_{1 \leq i \leq N}$ and $(\ell_{i(i+1)})_{1 \leq i \leq N-1}$ are invariant when reversing their orders:*

$$\forall 1 \leq i \leq N, \ell_i = \ell_{N-i+1} \quad \text{and} \quad \forall 1 \leq i \leq N-1, \ell_{i(i+1)} = \ell_{(N-i)(N-i+1)}.$$

Then, under the simplicity assumption Lemma 3.3, the eigenvectors $(\mathbf{a}_j)_{1 \leq j \leq N}$ of the eigenvalue problem (3.22) satisfy

$$\forall 1 \leq i \leq N, a_{ij} = (-1)^{k_j} a_{(N-i+1)j},$$

with $k_j = 0$ or $k_j = 1$.

Proof. This is an immediate consequence of the fact that under the symmetry assumption, $C_{ij}x_j = C_{ij}x_{N-1+j}$ and $V_{ij}x_j = V_{ij}x_{N-1+j}$ for any $x \in \mathbb{C}^N$. \square

Therefore, a system of resonators which is invariant by reversing the order of its elements attains in the limit $\delta \rightarrow 0$ perfect transmission at all its subwavelength resonances. We illustrate this property numerically by considering a system of six identical resonators, illustrated on Figure 15.

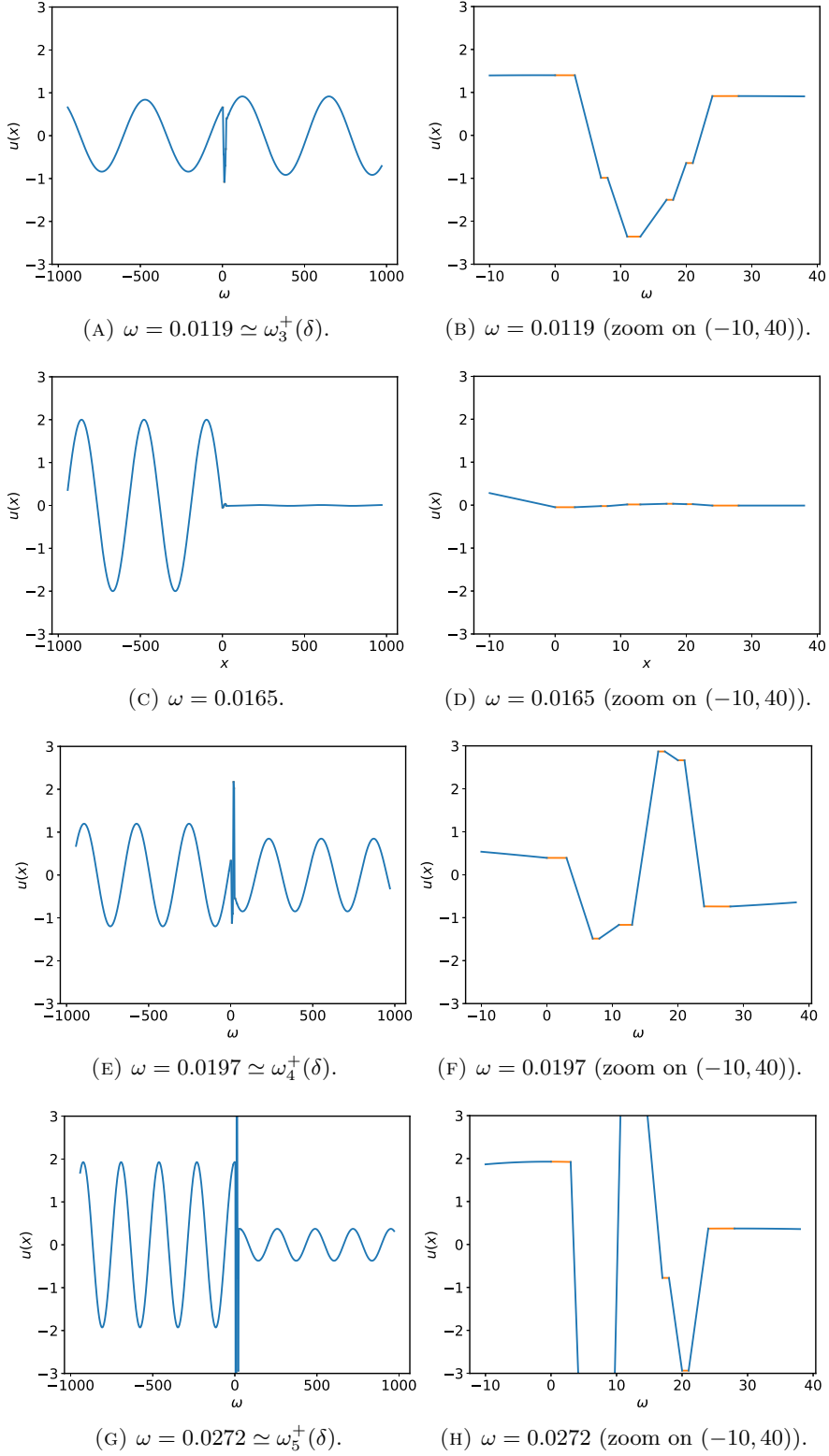


FIGURE 13. Wave solution $\Re(u(x)e^{-i\phi})$ to (1.7) for four incident frequencies $\omega \in \{0.0119, 0.0165, 0.0197, 0.0272\}$ in the six resonator setting of Section 5.4. These frequencies, reported with the red mark and the orange crosses on Figure 12), are either far from or close to the resonances. The part of the solution in the resonators is drawn in orange color. The phase ϕ is chosen according to (5.3).

The numerically computed transmission and reflection coefficients associated to the incident wave (5.2) are plotted on Figure 16. As in the previous Section 5.4, five resonant frequencies are visible in addition to the zero frequency $\omega_0(\delta) = 0$. However, the transmission coefficients are close to the values -1 and $+1$. They do not reach perfectly these values due to the fact that $\delta \neq 0$.

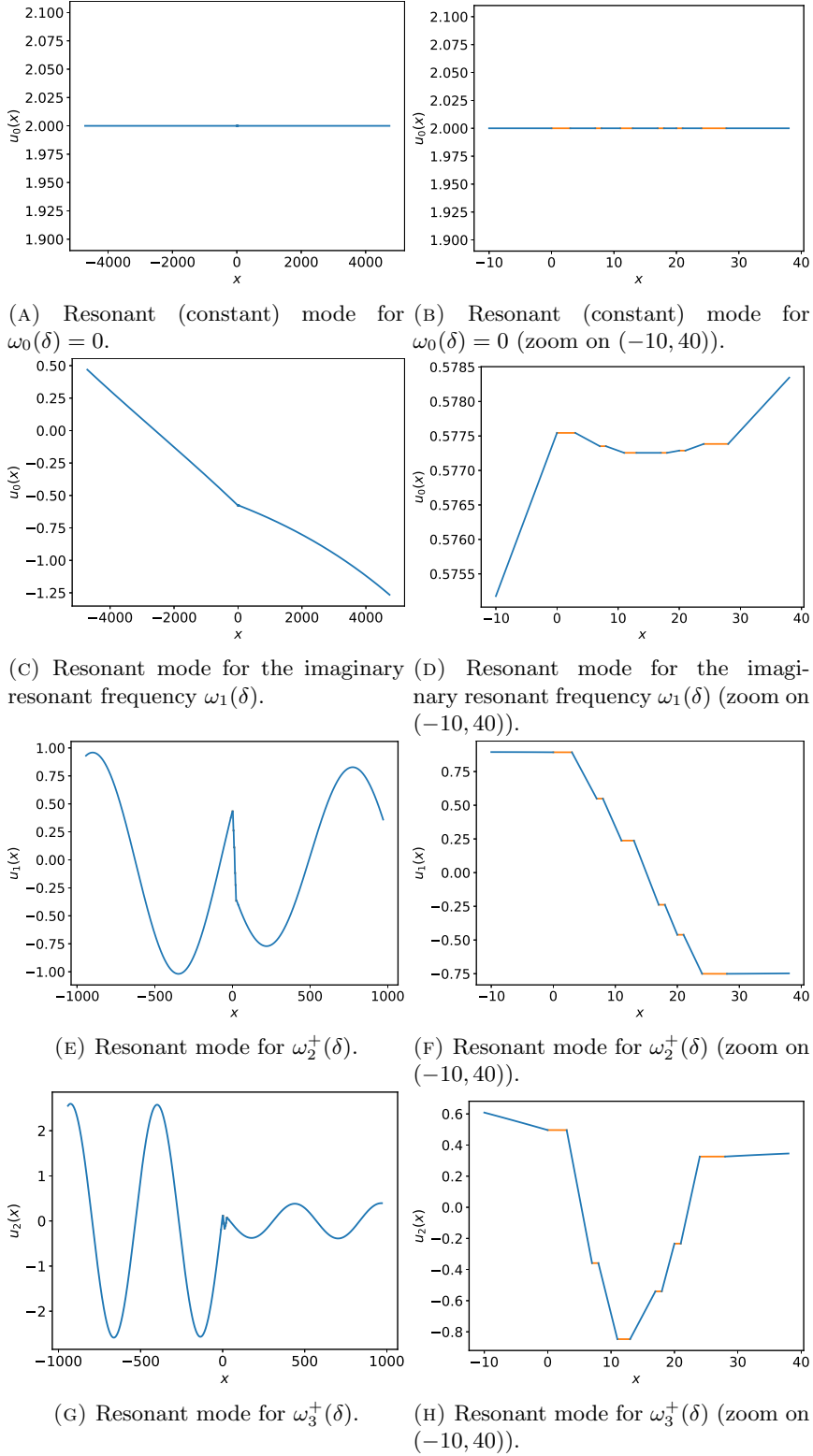


FIGURE 14. Subwavelength resonant modes for the six resonator case of Section 5.4.

The numerical values of the predicted subwavelength resonant frequencies and the scattering coefficients are reported in Table 4. We also report the predicted frequencies with orange crosses on the transmission and reflections plots of Figure 8. We observe that the location of the resonance is accurately predicted, but not the exact position of the maximum amplitude, which would require using higher order terms (of order $O(\delta^{\frac{3}{2}})$). We then plot on Figure 17 the total wave field generated by the incident wave (5.2) at the frequencies $\omega \in \{0.0446, 0.05, 0.0774, 0.0863\}$ which are alternatively close to $\omega_3^+(\delta)$, in between $\omega_3^+(\delta)$ and $\omega_4^+(\delta)$, and close to $\omega_4^+(\delta)$ and $\omega_6^+(\delta)$. Their values are indicated by the red mark and the orange crosses on Figure 16. In contrast with the previous Section 5.4, we observe that the transmitted fields are almost not attenuated at the

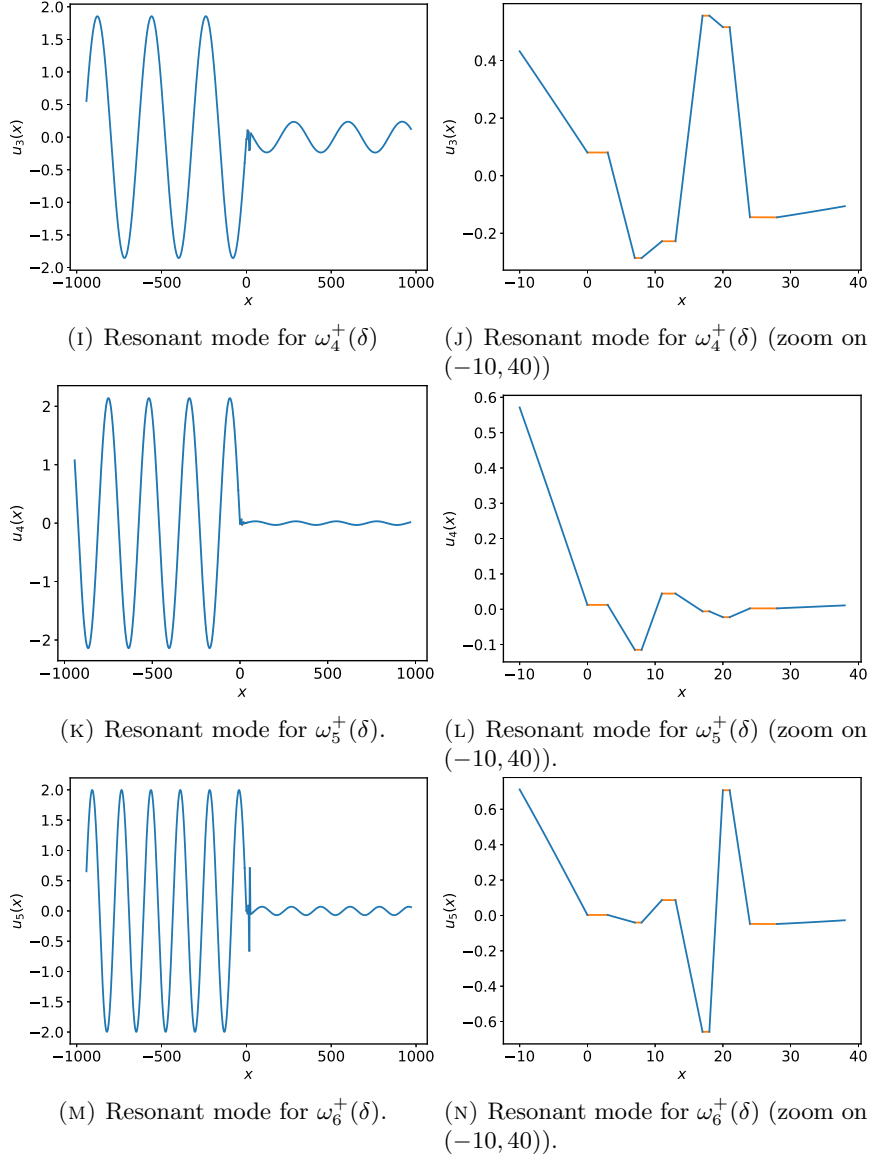


FIGURE 14. Subwavelength resonant modes for the two resonator case of Section 5.4.

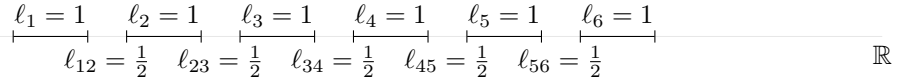


FIGURE 15. A symmetric system of six resonators considered in Section 5.5.

Frequency	Theoretical	Numerical	T	R
$\omega_0(\delta)$	0	0	1	0
$\omega_1(\delta)$	$-0.00033333i$	$-0.000333323i$	1	0
$\omega_2^+(\delta)$	$0.023149 - 0.000311i$	$0.023122 - 0.00031097i$	-1	0
$\omega_3^+(\delta)$	$0.044721 - 0.00025i$	$0.044676 - 0.00025012i$	1	0
$\omega_4^+(\delta)$	$0.063246 - 0.00016667i$	$0.063194 - 0.00016689i$	-1	0
$\omega_5^+(\delta)$	$0.07746 - 8.3333 \times 10^{-5}i$	$0.077412 - 8.3512 \times 10^{-5}i$	1	0
$\omega_6^+(\delta)$	$0.086395 - 2.2329 \times 10^{-5}i$	$0.086354 - 2.2391 \times 10^{-5}i$	-1	0

TABLE 4. Theoretical frequencies predicted by the leading-order approximation of Proposition 3.3 for the six resonator case of Section 5.4.

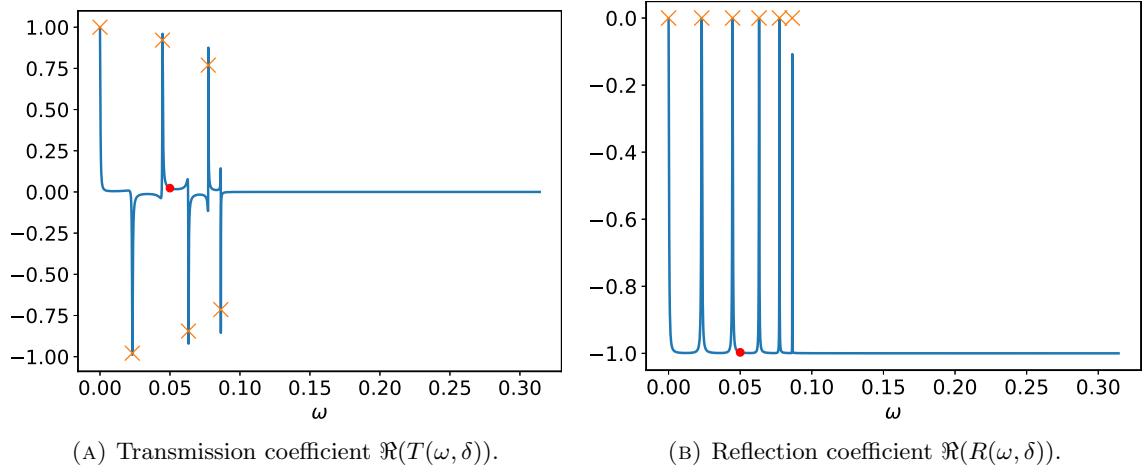


FIGURE 16. Transmission and reflection coefficients (Eq. (4.11)) for the symmetric six resonator case of Section 5.5. The red dot indicates the frequency $\omega = 0.05$, while the orange crosses indicates the predicted resonant frequencies (from Table 4). The wave solutions associated to the frequencies marked by the red dots and $\omega_3^+(\delta)$ and $\omega_4^+(\delta)$ are plotted on Figure 17.

highest order resonant frequencies, thereby achieving almost perfect transmission. Here, this system does not reach a positive reflection coefficient.

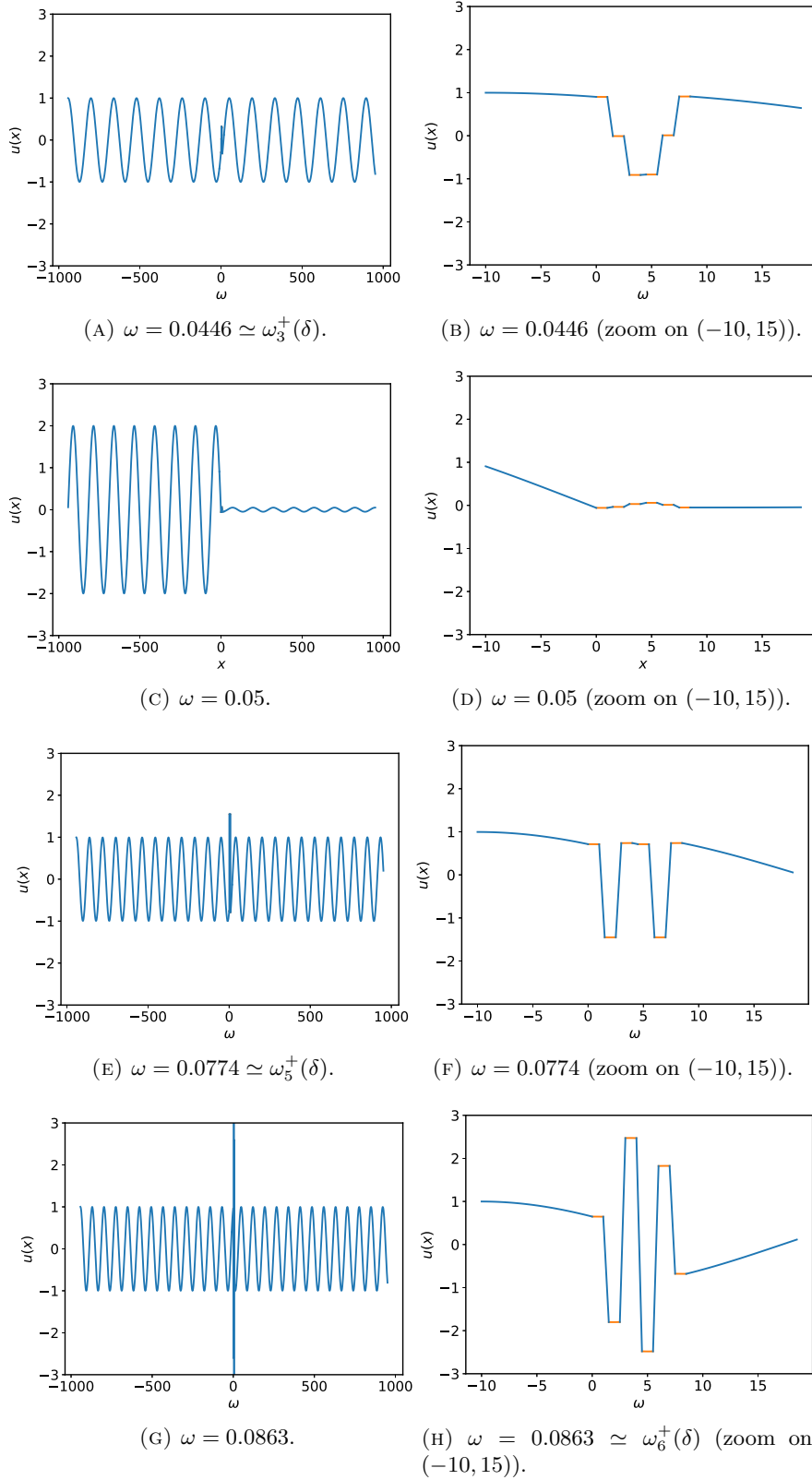


FIGURE 17. Wave solution $\Re(u(x)e^{-i\phi})$ to (1.7) for four incident frequencies $\omega \in \{0.0446, 0.05, 0.0774, 0.0863\}$ in the six resonator setting of Section 5.5. These frequencies, reported with the red mark and the orange crosses on Figure 16), are either far from or close to the resonances. The part of the solution in the resonators is drawn in orange color. The phase ϕ is chosen according to (5.3).

REFERENCES

- [1] H. AMMARI, G. CIRAOLO, H. KANG, H. LEE, AND G. W. MILTON, *Spectral theory of a Neumann–Poincaré-type operator and analysis of cloaking due to anomalous localized resonance*, *Archive for Rational Mechanics and Analysis*, 208 (2013), pp. 667–692.
- [2] H. AMMARI AND B. DAVIES, *Mimicking the active cochlea with a fluid-coupled array of subwavelength Hopf resonators*, *Proceedings of the Royal Society A*, 476 (2020), p. 20190870.
- [3] H. AMMARI, B. DAVIES, AND E. O. HILTUNEN, *Robust edge modes in dislocated systems of subwavelength resonators*, *Journal of the London Mathematical Society*, (2022), pp. 1–61, <https://doi.org/10.1112/jlms.12619>.
- [4] H. AMMARI, B. DAVIES, E. O. HILTUNEN, H. LEE, AND S. YU, *Wave interaction with subwavelength resonators*, arXiv preprint arXiv:2011.03575, (2020).
- [5] H. AMMARI, B. DAVIES, E. O. HILTUNEN, AND S. YU, *Topologically protected edge modes in one-dimensional chains of subwavelength resonators*, *Journal de Mathématiques Pures et Appliquées*, 144 (2020), pp. 17–49.
- [6] H. AMMARI, B. DAVIES, E. O. HILTUNEN, AND S. YU, *Topologically protected edge modes in one-dimensional chains of subwavelength resonators*, *Journal des Mathématiques Pures et Appliquées*, 144 (2020), pp. 17–49, <https://doi.org/10.1016/j.matpur.2020.08.007>.
- [7] H. AMMARI, F. FIORANI, AND E. O. HILTUNEN, *On the validity of the tight-binding method for describing systems of subwavelength resonators*, To appear in *Siam Journal on Applied Mathematics*, (2022).
- [8] H. AMMARI, B. FITZPATRICK, D. GONTIER, H. LEE, AND H. ZHANG, *Minnaert resonances for acoustic waves in bubbly media*, *Annales de l’Institut Henri Poincaré (C) Analyse Non Linéaire*, 35 (2018), pp. 1975–1998, <https://doi.org/10.1016/j.anihpc.2018.03.007>.
- [9] H. AMMARI, B. FITZPATRICK, H. KANG, M. RUIZ, S. YU, AND H. ZHANG, *Mathematical and Computational Methods in Photonics and Phononics*, vol. 235 of *Mathematical Surveys and Monographs*, American Mathematical Society, Providence, Rhode Island, oct 2018, <https://doi.org/10.1090/surv/235>.
- [10] R. CARMINATI, A. CAZÉ, D. CAO, F. PERAGUT, V. KRACHMALNICOFF, R. PIERRAT, AND Y. DE WILDE, *Electromagnetic density of states in complex plasmonic systems*, *Surface Science Reports*, 70 (2015), pp. 1–41, <https://doi.org/10.1016/j.surfrep.2014.11.001>.
- [11] J. CHRISTENSEN, L. MARTIN-MORENO, AND F. J. GARCIA-VIDAL, *Theory of resonant acoustic transmission through subwavelength apertures*, *Physical Review Letters*, 101 (2008), pp. 2–5, <https://doi.org/10.1103/PhysRevLett.101.014301>.
- [12] R. V. CRASTER AND B. DAVIES, *Asymptotic characterisation of localised defect modes: Su-Schrieffer-Heeger and related models*, arXiv preprint arXiv:2202.07324, (2022).
- [13] M. DEVAUD, T. HOCQUET, J. C. BACRI, AND V. LEROY, *The Minnaert bubble: An acoustic approach*, *European Journal of Physics*, 29 (2008), pp. 1263–1285, <https://doi.org/10.1088/0143-0807/29/6/014>.
- [14] C. L. FEFFERMAN, J. P. LEE-THORP, AND M. I. WEINSTEIN, *Honeycomb schrödinger operators in the strong binding regime*, *Communications on Pure and Applied Mathematics*, 71 (2018), pp. 1178–1270.
- [15] F. FEPPON AND H. AMMARI, *Modal decompositions and point scatterer approximations near the minnaert resonance frequencies*, *Studies in Applied Mathematics*, (2022), <https://doi.org/https://doi.org/10.1111/sapm.12493>.
- [16] F. FEPPON AND H. AMMARI, *Subwavelength resonant acoustic scattering in fast time-modulated media*. HAL preprint hal-03659025, May 2022.
- [17] W. A. HARRISON, *Electronic structure and the properties of solids: the physics of the chemical bond*, Courier Corporation, 2012.
- [18] P. HEIDER, D. BEREICHEZ, R. V. KOHN, AND M. I. WEINSTEIN, *Optimization of scattering resonances*, *Structural and Multidisciplinary Optimization*, 36 (2008), pp. 443–456, <https://doi.org/10.1007/s00158-007-0201-8>.
- [19] M. LANOY, R. PIERRAT, F. LEMOULT, M. FINK, V. LEROY, AND A. TOURIN, *Subwavelength focusing in bubbly media using broadband time reversal*, *Physical Review B*, 91 (2015), p. 224202.
- [20] F. LEMOULT, M. FINK, AND G. LEROSEY, *Acoustic resonators for far-field control of sound on a subwavelength scale*, *Physical Review Letters*, 107 (2011), p. 064301.
- [21] F. LEMOULT, N. KAINA, M. FINK, AND G. LEROSEY, *Soda cans metamaterial: A subwavelength-scaled phononic crystal*, *Crystals*, 6 (2016), p. 82, <https://doi.org/10.3390/cryst6070082>.
- [22] F. LEMOULT, N. KAINA, M. FINK, AND G. LEROSEY, *Soda cans metamaterial: a subwavelength-scaled phononic crystal*, *Crystals*, 6 (2016), p. 82.
- [23] V. LEROY, A. BRETAGNE, M. FINK, H. WILLAIME, P. TABELING, AND A. TOURIN, *Design and characterization of bubble phononic crystals*, *Applied Physics Letters*, 95 (2009), p. 171904.
- [24] V. LEROY, A. STRYBULEVYCH, M. LANOY, F. LEMOULT, A. TOURIN, AND J. H. PAGE, *Superabsorption of acoustic waves with bubble metascreens*, *Physical Review B*, 91 (2015), p. 020301.
- [25] H. LI, H. LIU, AND J. ZOU, *Minnaert resonances for bubbles in soft elastic materials*, *SIAM Journal on Applied Mathematics*, 82 (2022), pp. 119–141.
- [26] J. LIN AND F. SANTOSA, *Resonances of a finite one-dimensional photonic crystal with a defect*, *SIAM Journal on Applied Mathematics*, 73 (2013), pp. 1002–1019, <https://doi.org/10.1137/120897304>.
- [27] J. LIN AND H. ZHANG, *Mathematical theory for topological photonic materials in one dimension.*, arXiv preprint arXiv:2101.05966v2, (2021).
- [28] A. MANTILE, A. POSILICANO, AND M. SINI, *On the Origin of Minnaert Resonances*, arXiv preprint arXiv:2110.03043, (2021).
- [29] M. MINNAERT, *XVI. On musical air-bubbles and the sounds of running water*, *The London, Edinburgh, and Dublin Philosophical Magazine and Journal of Science*, 16 (1933), pp. 235–248.
- [30] D. E. MULLER, *A method for solving algebraic equations using an automatic computer*, *Mathematical tables and other aids to computation*, 10 (1956), pp. 208–215.
- [31] B. N. PARLETT, *The symmetric eigenvalue problem*, SIAM, 1998.
- [32] A. T. PAXTON ET AL., *An introduction to the tight binding approximation–implementation by diagonalisation*, *NIC Series*, 42 (2009), pp. 145–176.
- [33] D. A. THOMAS AND H. P. HUGHES, *Enhanced optical transmission through a subwavelength 1D aperture*, *Solid State Communications*, 129 (2004), pp. 519–524, <https://doi.org/10.1016/j.ssc.2003.11.029>.
- [34] O. VELIZ, *Muller’s method*, June 2022. <https://github.com/osveliz/numerical-veliz/blob/master/src/rootfinding/Muller.py>.

- [35] X. WANG, *Acoustical mechanism for the extraordinary sound transmission through subwavelength apertures*, Applied Physics Letters, 96 (2010), pp. 2008–2011, <https://doi.org/10.1063/1.3378268>.
- [36] D. ZHAO, M. XIAO, C. W. LING, C. T. CHAN, AND K. H. FUNG, *Topological interface modes in local resonant acoustic systems*, Physical Review B, 98 (2018), pp. 1–8, <https://doi.org/10.1103/PhysRevB.98.014110>.
- [37] M. ZWORSKI, *Mathematical study of scattering resonances*, Bulletin of Mathematical Sciences, 7 (2017), pp. 1–85, <https://doi.org/10.1007/s13373-017-0099-4>.